

Versatile Coordination of Acetazolamide to Ruthenium(II) *p*-Cymene Complexes and Preliminary Cytotoxicity Studies

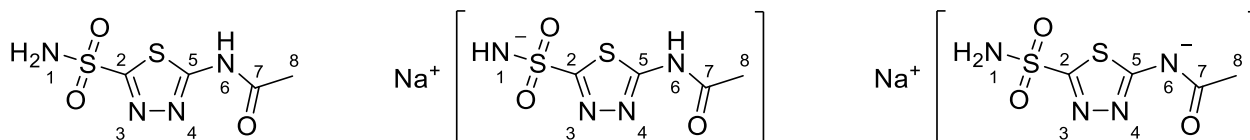
*Lorenzo Biancalana, Lucinda K. Batchelor, Gianluca Ciancaleoni, Stefano Zacchini, Guido Pampaloni,
Paul J. Dyson, Fabio Marchetti*

Supporting Information

<u>Table of contents</u>	<i>Page/s</i>
Synthesis and spectroscopic characterization of sodium acetazolamidate and spectroscopic characterization of acetazolamide (Chart S1)	S2
H-bond network present within the crystal structures of 1A ·0.5CH ₂ Cl ₂ and 5 ·H ₂ O (Figures S1-S2)	S3-S4
Table S1. k_r (in s ⁻¹) values for 1A/1B equilibrium derived from VT- ¹ H EXSY NMR experiments at different temperature (T, in K) and mixing time (τ_m , in s) values	S5
¹ H NMR spectra for the 1A/1B equilibrium in CD ₃ OD (Figures S3-S4)	S6-S7
DFT studies on the protonation of 5 (Figure S5)	S8
Other reactions of 5 with Brønsted acids or methylating reagents	S9
Stability studies in water and DMSO:water solutions (Tables S2-S3, Charts S2-S7)	S10-S16
Interconversion of [4] ⁺ , 5 and [6] ⁺ in D ₂ O (Chart S8; Figures S6-S8)	S17-S21
Solid-state IR spectra of Ru compounds (Figures S9-S15)	S22-S28
¹ H/ ¹³ C/ ¹⁴ N/ ³¹ P NMR spectra of Ru compounds (Figures S16-S36)	S29-S49
Notes and references	S50-S51

**Synthesis and spectroscopic characterization of sodium acetazolamidate, Na[AcmH], and
spectroscopic characterization of acetazolamide, AcmH₂**

Chart S1. Structures of **AcmH₂** (left) and **Na[AcmH]**, with negative charge on N1 (center) or N6 (right) atoms¹ (numbering refers to C and N atoms).



AcmH₂. IR (solid state): $\tilde{\nu}/\text{cm}^{-1}$ = 3323m-sh ($\nu_{\text{N-H}}$), 3304m ($\nu_{\text{N-H}}$), 3186w ($\nu_{\text{N-H}}$), 3105w ($\nu_{\text{N-H}}$), 3011w, 2904m, 2781m, 1684m ($\nu_{\text{C=O}}$), 1560m-sh (δ_{NH_2}), 1548s ($\nu_{\text{C=N}}$), 1435m, 1363s, 1313s ($\nu_{\text{as,SO}_2}$), 1282m, 1246m, 1167s ($\nu_{\text{s,SO}_2}$), 1119m, 1105w, 1086m, 1045w, 1011w, 972m, 922m-sh, 911m, 840m, 815m, 732w, 704w, 673m. ¹H NMR (DMSO-*d*₆): δ/ppm = 13.0 (s-br, 1H, N6-H), 8.32 (s-br, 2H, N1-H), 2.22 (s, 3H, C8-H). ¹³C{¹H} NMR (DMSO-*d*₆): δ/ppm = 169.8 (C7);² 164.5, 161.4 (C2 + C5), 22.6 (C8).

Na[AcmH]. A suspension of acetazolamide (76 mg, 0.34 mmol) in H₂O (2 mL) was treated with NaOH (1.0 M in H₂O; 0.34 mL, 0.34 mmol) then heated at 55 °C for 2 h, affording a colorless solution. Therefore, volatiles were removed under vacuum; the residue was dissolved in MeOH and filtered over celite. The filtrate was taken to dryness under vacuum and the resulting colorless solid was washed with Et₂O and dried under vacuum. Yield 83 mg, 99%. The compound is soluble in H₂O, DMSO and MeOH, poorly soluble in *i*PrOH and insoluble in Et₂O. IR (solid state): $\tilde{\nu}/\text{cm}^{-1}$ = 3479m, 3292s ($\nu_{\text{N-H}}$), 3159m ($\nu_{\text{N-H}}$), 3015m-sh, 2970s, 2930m, 2779m, 1706m ($\nu_{\text{C=O}}$), 1550s ($\nu_{\text{C=N}}$), 1428s, 1372s, 1344m, 1313m ($\nu_{\text{as,SO}_2}$), 1282w, 1255m-sh, 1238s, 1167s ($\nu_{\text{s,SO}_2}$), 1118s-sh, 1092s, 1034m-sh, 991s, 972m, 952s, 816m, 767m, 707m, 679s. ¹H NMR (DMSO-*d*₆): δ/ppm = 7.57 (s-br, 2H, N1-H), 1.96 (s, 3H, C8-H). ¹³C{¹H} NMR (DMSO-*d*₆): δ/ppm = 176.2 (C7); 171.9, 158.6 (C2 + C5), 26.4 (C8).

Figure S1. Partial representation of the H-bond network present within the crystal structure of **1A**·0.5CH₂Cl₂.

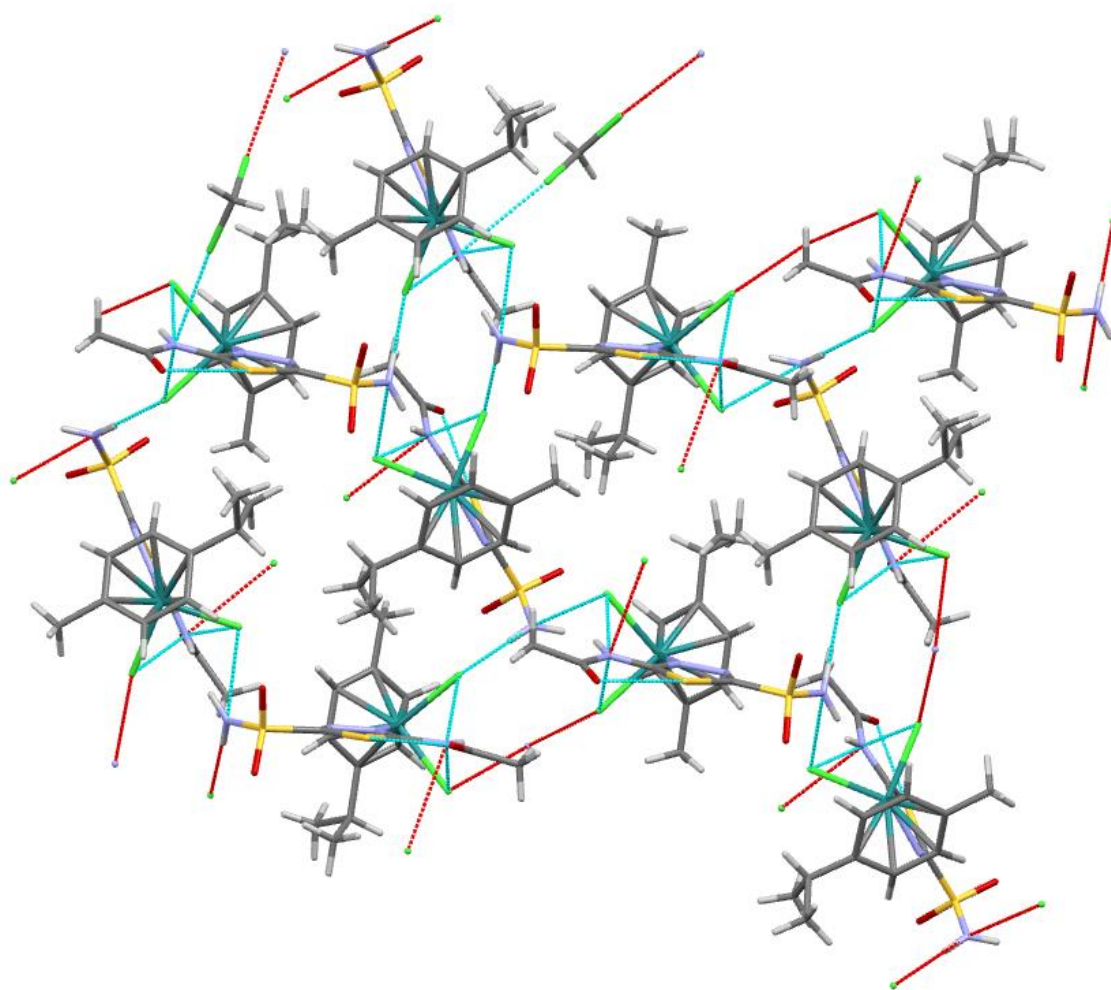


Figure S2. Partial representation of the H-bond network present within the crystal structure of **5**·H₂O.

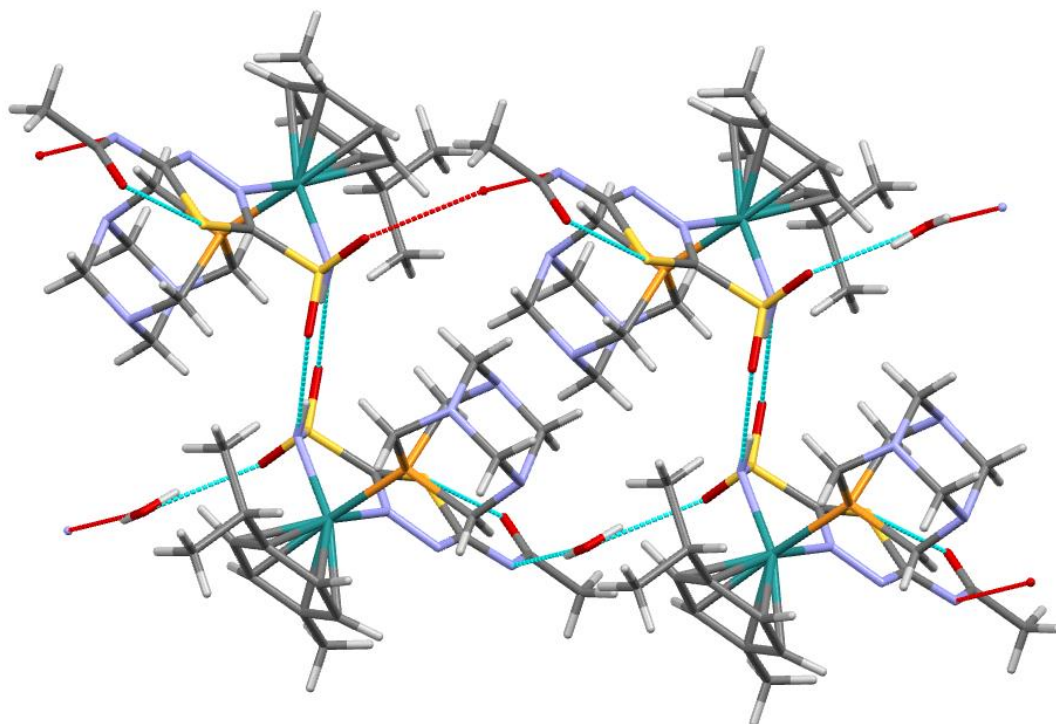


Table S1. k_r (in s^{-1}) values for **1A/1B** equilibrium derived from VT- 1H EXSY NMR experiments at different temperature (T, in K) and mixing time (τ_m , in s) values.

T	τ_m	k_r
298.6	0.4	0.32
308.2	0.4	0.95
317.2	0.4	1.69
317.2	0.2	1.43
323.2	0.2	3.72

Figure S3. ^1H NMR spectrum of the equilibrium mixture consisting of **1A**, **1B** and **2** (minor) after dissolution of **1A** in CD_3OD .

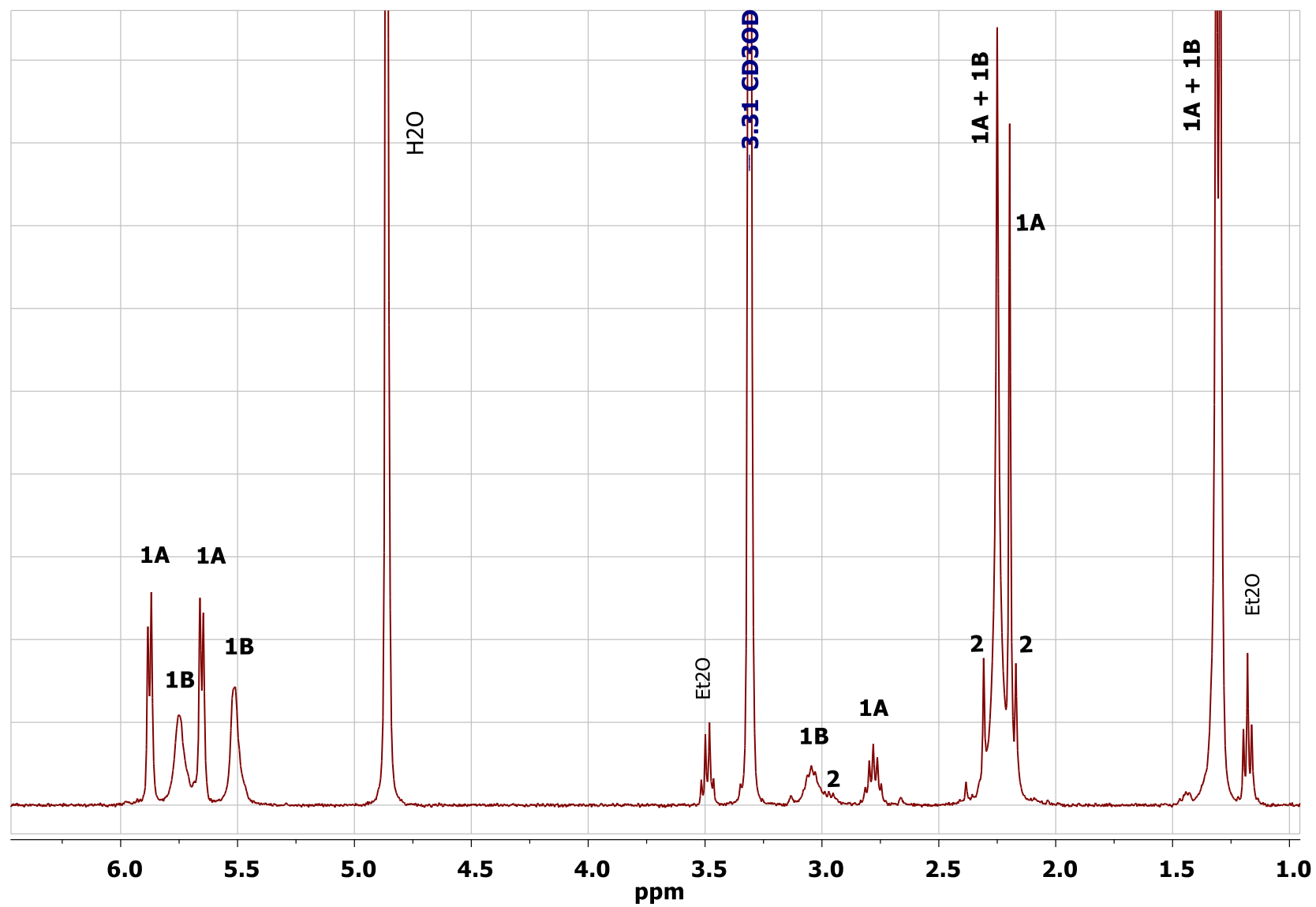
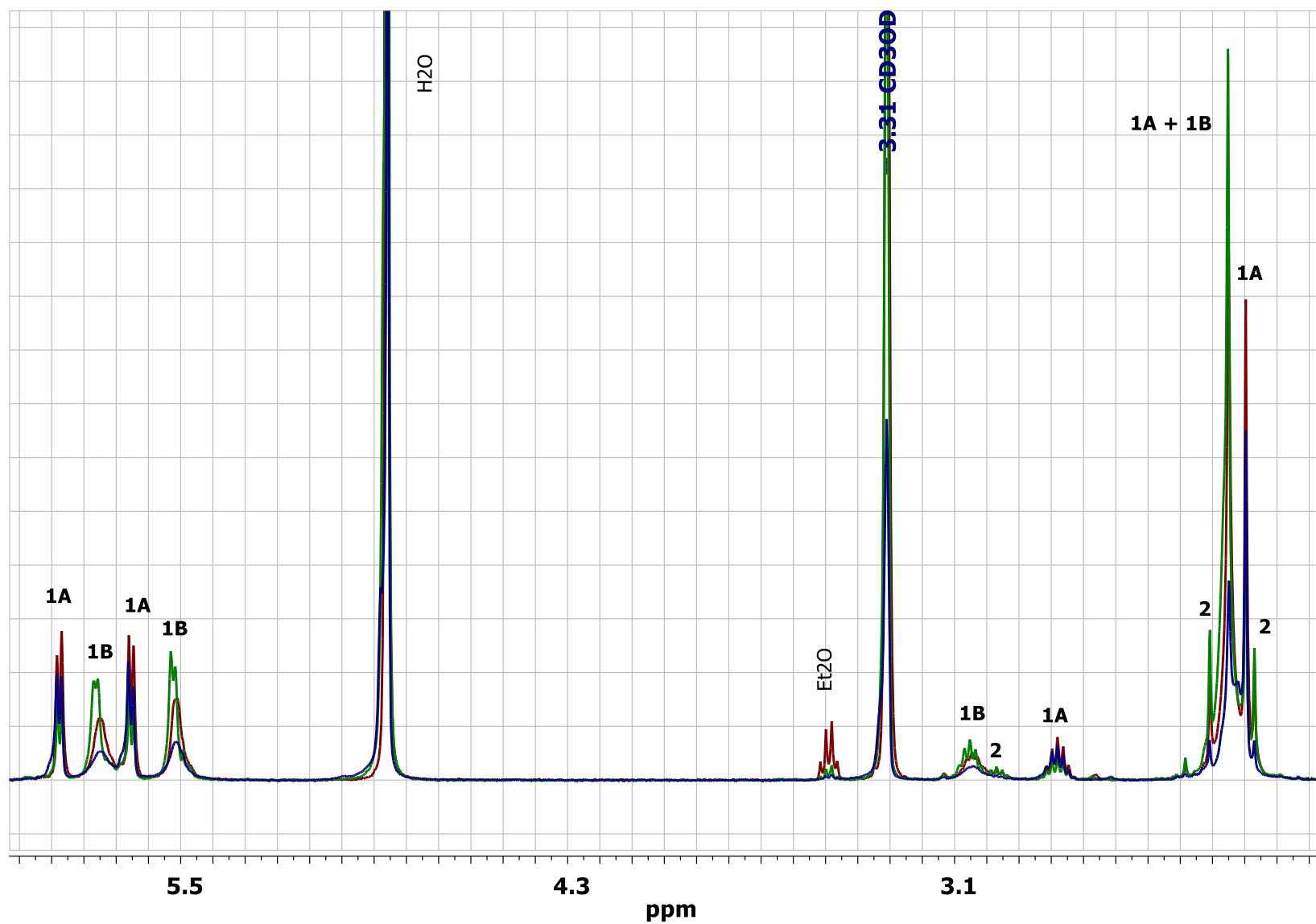
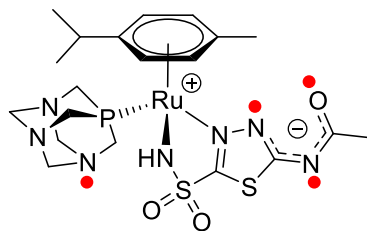


Figure S4. Comparison of ^1H NMR spectra of the equilibrium mixture consisting of **1A**, **1B** and **2** after dissolution of **1A** (red line), **1A** + AcM_2 (green line) and **1A** + $[(\eta^6\text{-}p\text{-cymene})\text{RuCl}(\mu\text{-Cl})_2]$ (blue line) in CD_3OD .



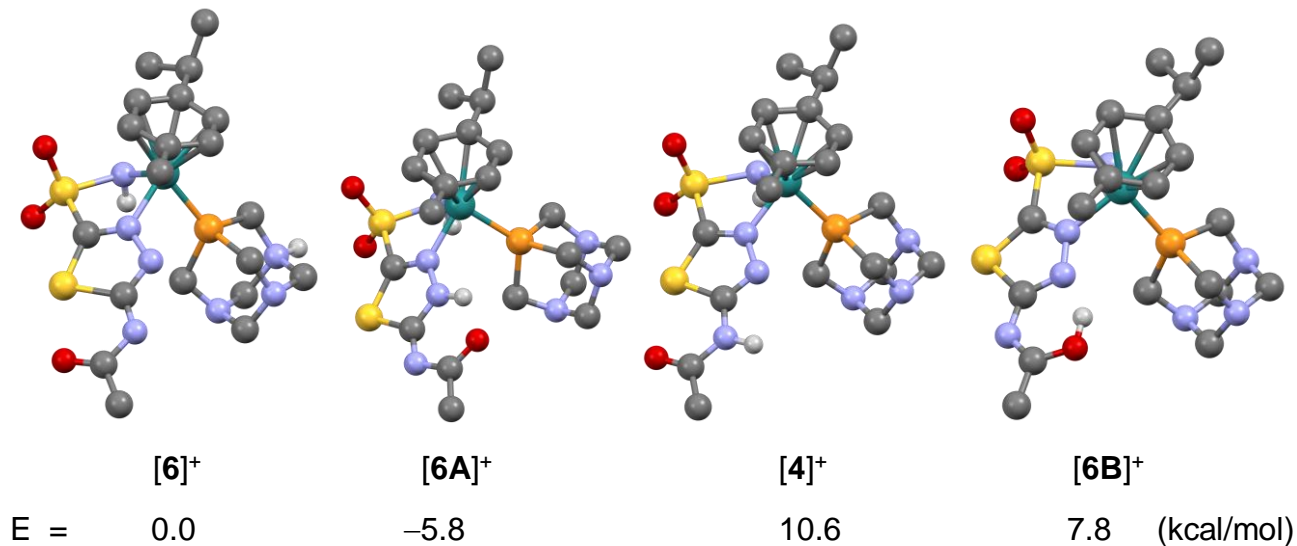
DFT studies on the protonation of **5**

Four possible sites for the H^+ attack to **5** have been considered (red dots):



The energy of each product has been DFT computed (Figure S5). The most stable isomer is not the experimentally observed $[\mathbf{6}]^+$, but $[\mathbf{6A}]^+$, since stabilizing intramolecular hydrogen bond is established with the oxygen atom. However, in methanol a large number of interactions between the solvent and the acid/basic centers of the molecule exist, making intramolecular interactions less important and the relative stability of the isomers hardly predictable without an accurate solvation model.

Figure S5. DFT-optimized geometries and energies of different isomers of $[\mathbf{6}]^+$. Level of theory: M06/def2-TZVP/methanol (cpcm)



Other reactions of **5** with Brønsted acids or methylating reagents

AcOH. A suspension of **5** (31 mg, 0.050 mmol) in MeOH (3 mL) was treated with AcOH (5 μ L, 0.09 mmol) then stirred at room temperature. After 5 h, the reaction mixture (yellow solution + solid) was filtered and the solid was washed with MeOH, Et₂O and dried under vacuum. The solid (9 mg, 29%) was identified as the starting material **5** by IR and NMR (¹H, ³¹P{¹H} in CD₃OD). The yellow filtrate solution contained a mixture of products (³¹P{¹H} NMR (CD₃OD): δ /ppm = -26.1, -26.2, -29.1, -30.6, -32.4, -108.8).

HNO₃. The reaction was carried out as described for the synthesis of [**6**]NO₃, using 2.0 equivalents of HNO₃. The progress of reaction was checked by ³¹P{¹H} NMR (δ /ppm = -23.5 only) then Et₂O was added to the reaction mixture, causing the precipitation of a yellow solid. The suspension was filtered, and the solid washed with Et₂O then dried under vacuum. The solid (33% yield) was identified as [**6**]NO₃ by NMR (¹H, ³¹P{¹H} in CD₃OD).

TsOH. The reaction was carried out as described for the synthesis of [**6**][TsO], using 2.0 equivalents of TsOH. A yellow-ocher solid was isolated, containing [**6**][TsO] and minor amounts of byproducts (¹H, ³¹P{¹H} NMR in CD₃OD).

MeOTf. In a 25-mL Schlenk tube under N₂, a suspension of **5** (55 mg, 0.090 mmol) in CH₂Cl₂ (6 mL) was treated with MeOTf (15 μ L, 0.13 mmol) then stirred at room temperature for 14 h. NMR analysis of the resulting solution revealed the formation of a mixture of products. ¹H NMR (CD₃OD): δ /ppm = 2.86, 2.53, 2.34, 2.31, 2.26 (s, CH₃). ³¹P{¹H} NMR (CD₃OD): δ /ppm = -4.50 (minor), -16.9, -17.0. Therefore MeOTf (50 μ L, 0.44 mmol) was added again and the reaction mixture was stirred for 14 h at room temperature. NMR analysis revealed the formation of a mixture of products. ³¹P{¹H} NMR (CD₃OD): δ /ppm = -10.7, -10.8, -11.1, -11.5.

MeI. The reaction was carried out as previously described for MeOTf, using MeI (15 μ L, 0.24 mmol). The starting material **5** was recovered after volatiles removal under vacuum (¹H, ³¹P{¹H} NMR in CD₃OD).

Stability studies in water and DMSO:water solutions

General procedure. The following stock solutions were used for the stability experiments: **a**, DMSO- d_6 /D $_2$ O 9:1 v/v; **b**, DMSO- d_6 /D $_2$ O 9:1 v/v + NaCl (0.11 M); **c**, DMSO- d_6 /D $_2$ O 8:5 v/v + NaCl (0.11 M); **d**, DMSO- d_6 /D $_2$ O 1:1 v/v + NaCl (0.11 M); **e**, D $_2$ O; **f**, D $_2$ O + NaCl (0.11 M) + Na $_2$ HPO $_4$ /NaH $_2$ PO $_4$ ($\Sigma c_{(PO_4)} = 5.1 \cdot 10^{-2}$ M, pD = 7.46³) (PBS, phosphate buffer saline solution). Dimethyl sulfone (Me $_2$ SO $_2$, *ca.* $5 \cdot 10^{-3}$ M) was added to each solution as a reference for ^1H NMR spectra⁴ ($\delta/\text{ppm} = 2.97$ (s, 6H) in **a-d**; 3.15 (s, 6H) in **e-f**). Ruthenium complexes were dissolved in the selected medium (**a-f**, 0.6 mL; $c_{\text{Ru}} = 12$ mM); the resulting solutions were maintained at 37 °C for 72 h and analyzed by ^1H and $^{31}\text{P}\{^1\text{H}\}$ NMR spectroscopy as a function of time. NMR measurements were performed upon brief cooling to ambient temperature and then the solutions were heated again at 37 °C. For water-soluble compounds ([**4**]NO $_3$, **5**, [**6**]NO $_3$), molar conductivity (Λ_m) and pH of a $2 \cdot 10^{-3}$ M solution in H $_2$ O were measured and additional stability experiments at reflux temperature in D $_2$ O were performed (see onward).

In D $_2$ O solutions, ^1H NMR chemical shifts were referenced to the residual HDO peak as in pure D $_2$ O ($\delta/\text{ppm} = 4.79$); in DMSO- d_6 :D $_2$ O mixtures, chemical shift were referenced to the residual (CHD $_2$)(CD $_3$)SO peak as in pure DMSO- d_6 ($\delta/\text{ppm} = 2.50$).⁵ Percent values of compounds in solution are based on ^1H NMR spectroscopy and refer to identified compounds only (indicated as “% NMR”) or refer to Me $_2$ SO $_2$ used as internal standard (indicated as “% NMR vs. *internal standard*”). NMR signals in braces {} indicate superimpositions with other signals in the same spectrum.

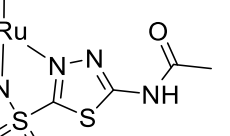
Reference data. $^1\text{H}/^{31}\text{P}\{^1\text{H}\}$ NMR spectra of the following compounds were recorded in D $_2$ O or in the appropriate DMSO- d_6 :D $_2$ O mixture and used for NMR assignments.

***p*-cymene.** ^1H NMR (DMSO- d_6 :D $_2$ O 9:1): $\delta/\text{ppm} = 7.12\text{--}7.02$ (m, 4H), 2.79 (hept, $J = 6.9$ Hz, 1H), 2.22 (s, 3H), 1.14 (d, $J = 6.9$ Hz, 6H). ^1H NMR (DMSO- d_6 :D $_2$ O 8:5): $\delta/\text{ppm} = 7.09\text{--}6.98$ (m, 4H),

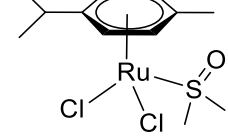
2.76–2.64 (m, 1H), 2.16 (s, 3H), 1.07 (d, $J = 6.8$ Hz, 6H). The compound is poorly soluble in the DMSO- d_6 :D $_2$ O 1:1 mixture. **pta**. ^1H NMR (D $_2$ O): $\delta/\text{ppm} = 4.53$ (pseudo-q, $^1J_{\text{HH}} = 12.9$ Hz, 6H), 3.98 (d, $^2J_{\text{HP}} = 8.9$ Hz, 6H). $^{31}\text{P}\{^1\text{H}\}$ NMR (D $_2$ O): $\delta/\text{ppm} = -98.5$. **AcmH $_2$** . ^1H NMR (DMSO- d_6 :D $_2$ O 9:1): $\delta/\text{ppm} = 2.23$ (s, 3H). ^1H NMR (DMSO- d_6 :D $_2$ O 8:5 and 1:1) $\delta/\text{ppm} = 2.19$ (s, 3H). **Na[AcmH]**. ^1H NMR (DMSO- d_6 :D $_2$ O 9:1): $\delta/\text{ppm} = 1.97$ (s, 3H). ^1H NMR (D $_2$ O): $\delta/\text{ppm} = 2.23$ (s, 3H).

Compound **1A** in DMSO- d_6 :D $_2$ O 9:1 + NaCl (**b**) and DMSO- d_6 :D $_2$ O 1:1 + NaCl (**d**). Orange solutions (0-72 h). Data are reported in Table S2, NMR detected species are shown in Chart S2. The set of signals for compound **2** in the DMSO- d_6 :D $_2$ O 1:1 solution (**d**) was identical to that observed for the same compound in the DMSO- d_6 :D $_2$ O 8:5 solution (see onward).

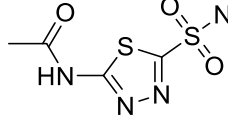
Chart S2 and Table S2. NMR detected species a function of time for DMSO- d_6 /D $_2$ O/NaCl solutions of **1A** at 37 °C.



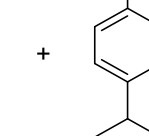
2



S



AcmH₂

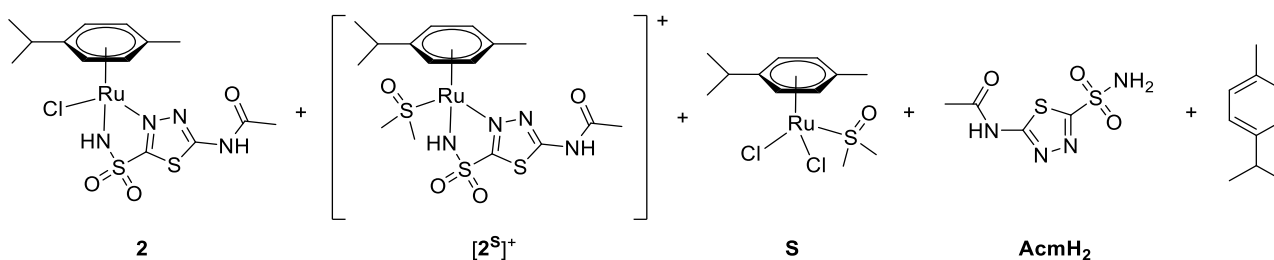


Solution		DMSO-d ₆ :D ₂ O 9:1 + NaCl (b)			DMSO-d ₆ :D ₂ O 1:1 + NaCl (d)		
time / h		0, 7.5	23, 47	72	0	8	24, 48, 72
% NMR	1A	0	0	0	0	0	0
	2	0	0	0	9	14	16
	S	50	49	48	46	43	42
	AcmH₂	50	50	50	45	43	42
	p-cymene	0	1	2	0	0	0

Compound **2** in DMSO-*d*₆:D₂O 9:1 ± NaCl (**a**, **b**) and DMSO-*d*₆:D₂O 8:5 + NaCl (**c**). Yellow solution (0-7 h in **a**, **b**; 0-72 h in **c**), orange solution (7-72 h in **a**, **b**). Data are reported in Table S3, NMR detected species are shown in Chart S3.

2. ¹H NMR (DMSO-*d*₆:D₂O 9:1, **a** / **b**): δ/ppm = 5.68–5.64 (m, 2H), 5.48–5.44 (m, 2H), 2.80 (hept, *J* = 6.8 Hz, 1H), 2.19 (s, 3H), 2.03 (s, 3H), 1.19 (d, *J* = 6.9 Hz, 6H). ¹H NMR (DMSO-*d*₆:D₂O 8:5, **c**): δ/ppm = 5.65 (d, *J* = 6.9 Hz, 1H), 5.61 (d, *J* = 5.8 Hz, 1H), 5.49 (d, *J* = 5.5 Hz, 1H), 5.41 (d, *J* = 6.0 Hz, 1H), 2.72 (hept, *J* = 6.8 Hz, 1H), 2.18 (s, 3H), 1.97 (s, 3H), 1.13 (d, *J* = 6.9 Hz, 6H).

Chart S3 and **Table S3.** NMR detected species a function of time for DMSO-*d*₆/D₂O ± NaCl solutions of **2** at 37 °C.



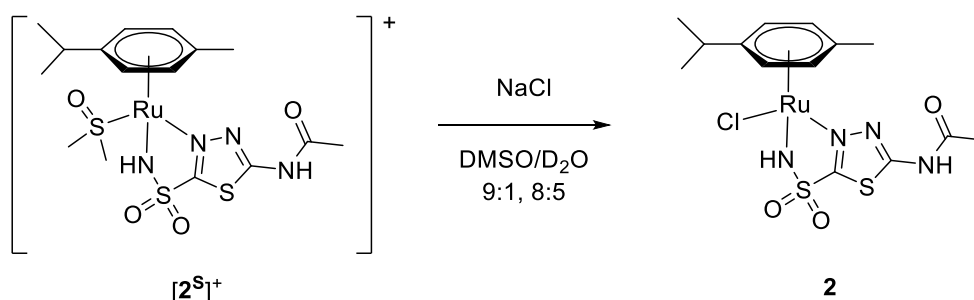
Solution		DMSO- <i>d</i> ₆ :D ₂ O 9:1 (+ NaCl); a (b)				
time / h		0	7.5	≈ 24.5	47.5	72
% NMR	vs. internal standard, 2	92 (79)	55 (55)	52 (55)	52 (52)	44 (50)
	2	86 (65)	43 (39)	41 (39)	41 (38)	36 (35)
	[2^S]⁺ ⁶	0 (0)	7 (0)	5 (0)	5 (0)	4 (0)
	S	8 (17)	26 (30)	26 (30)	24 (29)	23 (28)
	AcMH₂	6 (18)	22 (30)	23 (30)	21 (30)	24 (31)
	<i>p</i>-cymene	0 (0)	2 (1)	5 (2)	9 (4)	13 (6)
Solution		DMSO- <i>d</i> ₆ :D ₂ O 8:5 + NaCl (c)				
time / h		0	7	25.5	49	73
% NMR	vs. internal standard, 2	76	72	68	68	65
	2	66	61	61	61	59
	[2^S]⁺	7	6	5	5	6
	S	14	17	19	18	18
	AcMH₂	13	16	14	15	15
	<i>p</i>-cymene	0	0	1	1	2

Compound **3** in DMSO-*d*₆:D₂O 9:1 (**a**) and DMSO-*d*₆:D₂O 8:5 (**c** without NaCl). A similar set of ¹H NMR signals was observed in the two yellow solutions, which was attributed to the formation of [(η⁶-*p*-cymene)Ru(κ²*N,N'*-Ac₂H)(κS-DMSO)]⁺ (**[2^S]⁺**, Chart S4).

[2^S]⁺. ¹H NMR (DMSO-*d*₆:D₂O 9:1, **a**): δ/ppm = 6.11 (d, *J* = 5.9 Hz, 1H), 6.09–6.04 (m, 3H), 2.83 (hept, *J* = 7.0 Hz, 1H), 2.22 (s, 6H), 1.25 (d, *J* = 6.9 Hz, 3H), 1.18 (d, *J* = 6.7 Hz, 3H). ¹H NMR (DMSO-*d*₆:D₂O 8:5, **c** without NaCl): δ/ppm = 6.05–6.00 (m, 2H), 5.99–5.94 (m, 2H), 2.78–2.70 (m, 1H), 2.22 (s, 3H), 2.17 (s, 3H), 1.18–1.10 (m, 6H).

Addition of excess NaCl to these solutions led to the disappearance of **[2^S]⁺** and formation of **2** and **S** (¹H NMR spectra identical to those of **2** dissolved in DMSO-*d*₆:D₂O 9:1 and 8:5, respectively)

Chart S4. NMR detected species for DMSO-*d*₆/D₂O solutions of **3**; formation of **2** upon addition of NaCl.

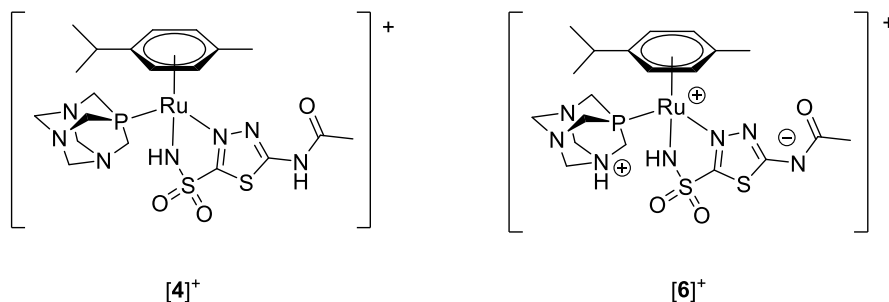


Compounds **[4]NO₃** and **[6]NO₃** in D₂O (**e**). Yellow solutions (0-72 h). A single set of ¹H and ³¹P{¹H} NMR signals was observed, attributed to the starting material (**[4]**⁺ or **[6]**⁺, respectively, Chart S5). No changes in ¹H and ³¹P{¹H} NMR spectra were observed after 72 h at 37 °C. Subsequent heating at reflux temperature for 1 h caused partial degradation (ca. 35% with respect to the initial amount of **[4]NO₃**; ca. 50% for **[6]NO₃**), with formation of AcOH, pta oxide (O=pta) and other unidentified products.

[4]NO₃. Λ_m (c = 2.4·10⁻³ M, H₂O): 139 S·cm²·mol⁻¹. pH (c = 2.4·10⁻³ M, H₂O) = 4.3. ¹H NMR (D₂O, **e**): δ/ppm = 6.15 (d, *J* = 6.3 Hz, 1H), 6.09 (d, *J* = 6.1 Hz, 1H), 6.07–6.03 (m, 2H), 4.57–4.51 (m, 6H), 4.18 (dd, *J* = 14.9, 2.1 Hz, 3H), 3.98 (dd, *J* = 15.2, 1.9 Hz, 3H), 2.69 (hept, *J* = 6.9 Hz, 1H), 2.36 (s, 3H), 2.14 (s, 3H), 1.27 (d, *J* = 6.7 Hz, 3H), 1.16 (d, *J* = 6.8 Hz, 3H). ³¹P{¹H} NMR (D₂O, **e**): δ/ppm = – 31.4. **Other products** (thermal degradation). ¹H NMR (D₂O, **e**): δ/ppm = 4.41 (d), 4.27 (d), 4.05 (d), 2.05 (s, AcOH). ³¹P{¹H} NMR (D₂O, **e**): δ/ppm = – 2.9 (O=pta⁷).

[6]NO₃. Λ_m (c = 2.2·10⁻³ M, H₂O) = 247 S·cm²·mol⁻¹. pH (c = 2.2·10⁻³ M, H₂O) = 3.1. ¹H NMR (D₂O, **e**): δ/ppm = 6.21 (d, *J* = 6.5 Hz, 1H), 6.11 (m-br, 3H), 4.72 (m/AB spin system, *J* = 13.7 Hz, 6H), 4.26 (d, *J* = 15.2 Hz, 3H), 4.11 (d, *J* = 15.7 Hz, 3H), 2.72 (hept, *J* = 6.7 Hz, 1H), 2.38 (s, 3H), 2.17 (s, 3H), 1.29 (d, *J* = 6.9 Hz, 3H), 1.19 (d, *J* = 6.9 Hz, 3H). ³¹P{¹H} NMR (D₂O, **e**): δ/ppm = – 27.6. **Other products** (thermal degradation). ¹H NMR (D₂O, **e**): δ/ppm = 5.79 (d), 5.56 (d), 4.53 (d), 4.21 (d), 3.27 (s), 3.24 (s), 3.21 (s), 3.19 (s), 2.59 (s), 2.08 (s, AcOH), 1.22 (d). ³¹P{¹H} NMR (D₂O, **e**): δ/ppm = 45.4, – 3.1 (O=pta⁷), – 26.8.

Chart S5. Structures of **[4]**⁺ and **[6]**⁺, NMR detected in the respective D₂O solution.



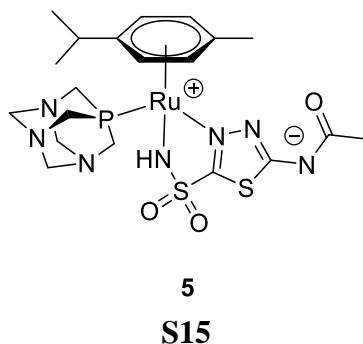
Compound 5 in D₂O (e). Yellow solution + solid (0-72 h); compound **5** is not completely soluble under the selected conditions. The solubility, calculated by ¹H NMR with respect to Me₂SO₂ (internal standard), is 8.5·10⁻³ M. A single set of ¹H and ³¹P{¹H} NMR signals was observed, attributed to the starting material (**5**, Chart S6). No changes in ¹H and ³¹P{¹H} NMR spectra were observed after 72 h at 37 °C.

5. Λ_m ($c = 1.7 \cdot 10^{-3}$ M, H_2O): $71 \text{ S} \cdot \text{cm}^2 \cdot \text{mol}^{-1}$. ^1H NMR (D_2O , **e**): $\delta/\text{ppm} = 6.11$ (d, $J = 6.3$ Hz, 1H), 6.09–6.04 (m, 2H), 6.00 (d, $J = 5.8$ Hz, 1H), 4.51 (m/AB spin system, 6H), 4.18 (dd, $J = 15.1, 2.6$ Hz, 3H), 3.95 (dd, $J = 15.1, 2.7$ Hz, 3H), 2.69 (hept, $J = 6.9$ Hz, 1H), 2.30 (s, 3H), 2.14 (s, 3H), 1.26 (d, $J = 6.9$ Hz, 3H), 1.14 (d, $J = 6.9$ Hz, 3H). $^{31}\text{P}\{^1\text{H}\}$ NMR (D_2O , **e**): $\delta/\text{ppm} = -31.3$.

Compounds **[4]NO₃**, **5** and **[6]NO₃** in D₂O + PBS (f). Yellow solution + solid (0-72 h). NMR spectra of the three solutions were identical: a single set of ¹H and ³¹P{¹H} NMR signals was observed, attributed to compound **5** (Chart S6).⁸ Under these conditions, the solubility of **5**, calculated by ¹H NMR with respect to Me₂SO₂ (internal standard), is 9.9·10⁻³ M. No changes in ¹H and ³¹P{¹H} NMR spectra were observed after 72 h at 37 °C.

5. ^1H NMR (D_2O , **f**): $\delta/\text{ppm} = 6.11\text{--}6.07$ (m, 3H), 5.98 (d, $J = 5.6$ Hz, 1H), 4.52 (m/AB spin system, $J = 14$ Hz, 6H), 4.19 (dd, $J = 15.1, 2.9$ Hz, 3H), 3.94 (dd, $J = 15.1, 2.9$ Hz, 3H), 2.70 (d, $J = 6.7$ Hz, 1H), 2.25 (s, 3H), 2.15 (s, 3H), 1.26 (d, $J = 6.9$ Hz, 3H), 1.14 (d, $J = 6.9$ Hz, 3H). $^{31}\text{P}\{^1\text{H}\}$ NMR (D_2O , **f**): $\delta/\text{ppm} = -31.2$.

Chart S6. NMR detected species for D₂O solution of **5** and D₂O + PBS solutions of [**4**]⁺NO₃⁻, **5** and [**6**]⁺NO₃⁻.

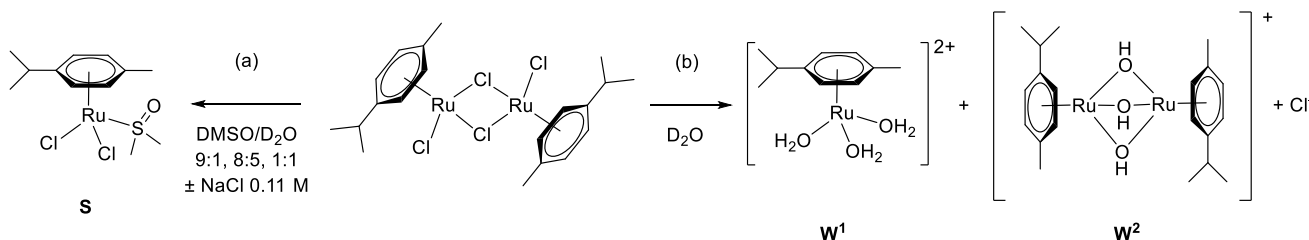


Compound $[(\eta^6\text{-}p\text{-cymene})\text{RuCl}(\mu\text{-Cl})]_2$ in $\text{DMSO}:\text{D}_2\text{O}$ mixtures **a-d**. Orange solutions. Quantitative formation of $[(\eta^6\text{-}p\text{-cymene})\text{RuCl}_2(\kappa\text{S-DMSO})]$ (**S**, Chart S7a) occurs in DMSO-d_6 and $\text{DMSO-d}_6:\text{D}_2\text{O}$ 9:1 \pm NaCl (**a**, **b**) solutions.⁹ A similar set of signals was observed in the $\text{DMSO-d}_6:\text{D}_2\text{O}$ 8:5 + NaCl (**c**) and $\text{DMSO-d}_6:\text{D}_2\text{O}$ 1:1 + NaCl (**d**) solutions, thus attributed to **S**.

S. ^1H NMR ($\text{DMSO-d}_6:\text{D}_2\text{O}$ 9:1, **a** / **b**): δ/ppm = 5.78 (d, J = 6.2 Hz, 2H), 5.73 (d, J = 6.2 Hz, 2H), 2.78 (hept, J = 6.8 Hz, 1H), 2.06 (s, 3H), 1.16 (d, J = 6.9 Hz, 6H). ^1H NMR ($\text{DMSO-d}_6:\text{D}_2\text{O}$ 8:5, **c** or 1:1, **d**): δ/ppm = 5.72 (d, J = 5.9 Hz, 2H), 5.67 (d, J = 5.6 Hz, 2H), 2.74–2.66 (m, 1H), 2.02 (s, 3H), 1.12 (d, J = 6.7 Hz, 6H). No change in the ^1H NMR spectra of solutions **c** and **d** was observed after 20 h at 37 °C.

$[(\eta^6\text{-}p\text{-cymene})\text{RuCl}_2]$ in D_2O (**e**). Yellow solution. The compound undergoes Ru-Cl hydrolysis with formation of $[(\eta^6\text{-}p\text{-cymene})\text{Ru}(\text{H}_2\text{O})_3]^{2+}$ (**W**¹), $[(\eta^6\text{-}p\text{-cymene})_2\text{Ru}_2(\mu\text{-OH})_3]^+$ (**W**²) and other species (Chart S7b).¹⁰ ^1H NMR (D_2O): δ/ppm = 5.99 (d, J = 6.3 Hz), 5.86 (d, J = 5.8 Hz, **W**¹), 5.74 (d, J = 5.6 Hz), 5.64 (d, J = 5.6 Hz, **W**¹), 5.53 (d, J = 5.7 Hz, **W**²), 5.32 (d, J = 5.4, **W**²), 2.88 (hept, J = 6.8 Hz, **W**¹ + **W**²), 2.76–2.64 (m), 2.25 (s), 2.21 (s, **W**¹), 2.12 (s, **W**²), 1.35 (d, J = 7.4 Hz), 1.33 (d, J = 7.0 Hz, **W**¹), 1.24 (d, J = 6.9). ^{35}Cl NMR (D_2O): δ/ppm = 0.63 ($\Delta\nu_{1/2}$ = 25 Hz, Cl^-). Minor variations in the ^1H spectrum were observed after 20 h at 37 °C. Addition of NaCl (0.1 M) to the solution caused broadening of ^1H NMR resonances.^{10b}

Chart S7. NMR detected species for $\text{DMSO-d}_6/\text{D}_2\text{O} \pm \text{NaCl}$ (**a**) or D_2O (**b**) solutions of $[(\eta^6\text{-}p\text{-cymene})\text{RuCl}_2]$.



Interconversion of [4]⁺, 5 and [6]⁺ in D₂O solution

General procedure. A solution of [4]NO₃ in D₂O (5.0 mg in 0.5 mL; c_{Ru} = 15 mM) was analyzed by ¹H and ³¹P{¹H} NMR then treated with excess Na₂CO₃ (6.2 mg, ca. 0.06 mmol) at room temperature. NMR spectra were repeated on the resulting yellow solution then HNO₃ (65% solution in H₂O, 10 μL, ca. 0.15 mmol) was added. When the evolution of CO₂ had ceased, NMR spectra were repeated. The procedure above described was then applied to compound [6]NO₃ (5.0 mg in 0.5 mL; c_{Ru} = 15 mM) and to a mixture of [4]NO₃ and [6]NO₃ in the same solution (2.2 mg each, separately dissolved in 0.3 mL D₂O then mixed, c_{Ru} = 13 mM).¹¹ NMR spectra of the three solutions after Na₂CO₃ addition were identical: a single set of ¹H and ³¹P{¹H} NMR signals was observed, due to the formation of 5.¹² Also following HNO₃ addition, identical NMR spectra were observed for the three solutions, suggesting the (re-)formation of [6]⁺.¹³ NMR data are reported below (those for D₂O solutions of [4]NO₃ and [6]NO₃ were previously reported, see page S10); NMR detected species are shown in Chart S8; NMR spectra are shown in Figures S2-S4.

Mixture of [4]NO₃ and [6]NO₃ in D₂O (ca. 1:1). Yellow solution. A single set of ¹H and ³¹P{¹H} NMR signals was observed, having intermediate chemical shift values between those of [4]NO₃ and [6]NO₃ in D₂O. No changes in ¹H and ³¹P{¹H} NMR spectra were observed after 48 h at 37 °C. Subsequent heating at reflux temperature for 1 h caused partial degradation, with formation of AcOH, pta oxide (O=pta) and other unidentified products.

[4]NO₃ + [6]NO₃ (single set, rapid exchange). ¹H NMR (D₂O): δ/ppm = 6.18 (d, *J* = 5.5 Hz, 1H), 6.10–6.07 (m, 3H), 4.63–4.53 (m/AB spin system, *J* = 13.5 Hz, 6H), 4.21 (d, *J* = 15.6 Hz, 3H), 4.03 (d, *J* = 15.4 Hz, 3H), 2.70 (hept, *J* = 6.8 Hz, 1H), 2.39 (s, 3H), 2.15 (s, 3H), 1.29 (d, *J* = 6.9 Hz, 3H), 1.18 (d, *J* = 6.8 Hz, 3H). ³¹P{¹H} NMR (D₂O): δ/ppm = – 30.6 ppm. **Other products** (thermal

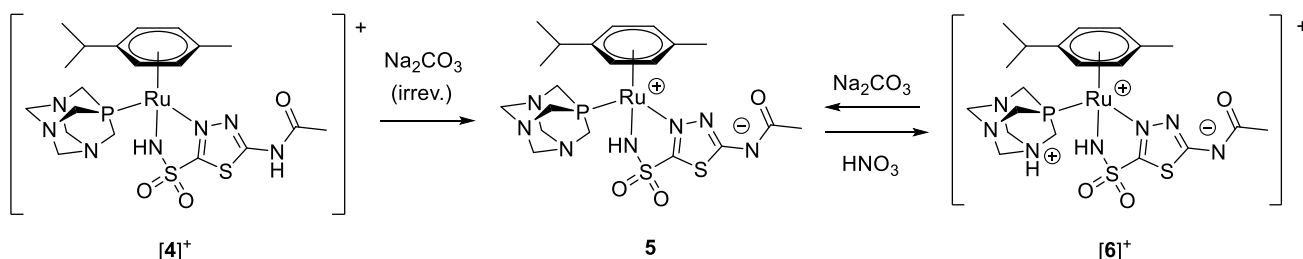
degradation). ^1H NMR (D_2O): 6.74-6.62 (m), 4.46-4.41 (m), 4.35-4.27 (m), 4.06 (d), 3.26 (d), 2.59 (s), 2.30 (s), 2.08 (s, AcOH), 1.86 (s), 0.87 (d). $^{31}\text{P}\{^1\text{H}\}$ NMR (D_2O): $\delta/\text{ppm} = -2.9$ ($\text{O}=\text{pta}^7$)

*Addition of Na_2CO_3 : formation of **5**.* ^1H NMR (D_2O): $\delta/\text{ppm} = 6.12\text{--}6.02$ (m, 3H), 5.93 (d, $J = 5.7$ Hz, 1H), 4.56–4.46 (m/AB system, $J = 14$ Hz, 6H), 4.17 (d, $J = 15.2$ Hz, 3H), 3.91 (d, $J = 13.8$ Hz, 3H), 2.69 (hept, $J = 6.6$ Hz, 1H), 2.21 (s, 3H), 2.14 (s, 3H), 1.25 (d, $J = 6.9$ Hz, 3H), 1.12 (d, $J = 6.9$ Hz, 3H). $^{31}\text{P}\{^1\text{H}\}$ NMR (D_2O): $\delta/\text{ppm} = -31.2$.

Addition of HNO_3 : formation of $[\mathbf{6}]^+$. ^1H NMR (D_2O): $\delta/\text{ppm} = 6.23$ (d, $J = 6.5$ Hz, 1H), 6.17–6.10 (m, 3H), 4.90* (s), 4.35 (dd, $J = 15.4, 2.2$ Hz, 3H), 4.22 (dd, $J = 15.3, 2.3$ Hz, 3H), 2.71 (hept, $J = 6.9$ Hz, 1H), 2.36 (s, 3H), 2.16 (s, 3H), 1.27 (d, $J = 6.9$ Hz, 3H), 1.17 (d, $J = 6.9$ Hz, 3H).

*Superimposed on HDO signal. $^{31}\text{P}\{^1\text{H}\}$ NMR (D_2O): $\delta/\text{ppm} = -23.5$.

Chart S8. Proposed acid-base reactions between $[\mathbf{4}]^+$, **5** and $[\mathbf{6}]^+$ in D_2O solution.



In a separate experiment, pta (1.4 mg) was added to a solution of $[\mathbf{4}]\text{NO}_3$ (6.0 mg, ca. 1:1 mol. ratio) in D_2O (0.5 mL). Two set of ^1H and $^{31}\text{P}\{^1\text{H}\}$ NMR signals were observed, in accordance with the formation of **5** (eq. S1).



5. ^1H and $^{31}\text{P}\{^1\text{H}\}$ NMR signals were identical to those of a D_2O solution of **5** (see page S11).

$[\text{ptaH}]\text{NO}_3$. ^1H NMR (D_2O): $\delta/\text{ppm} = 4.67$ (pseudo-q, $J = 13.0$ Hz, 6H), 4.04 (d, $J = 9.0$ Hz, 6H).

$^{31}\text{P}\{^1\text{H}\}$ NMR (D_2O): $\delta/\text{ppm} = -95.5$.

Figure S6. ^1H NMR spectra (3.70-6.50 ppm region) of $[\mathbf{4}]\text{NO}_3$ (a, violet line), $\mathbf{5}$ (b, blue line), $[\mathbf{6}]\text{NO}_3$ (c, cyan line) in D_2O , $\mathbf{5}$ in D_2O + PBS solution (d, green line), $[\mathbf{4}]^+/\text{D}_2\text{O}$ after Na_2CO_3 addition (e, yellow line) and after subsequent HNO_3 addition (f, red line).

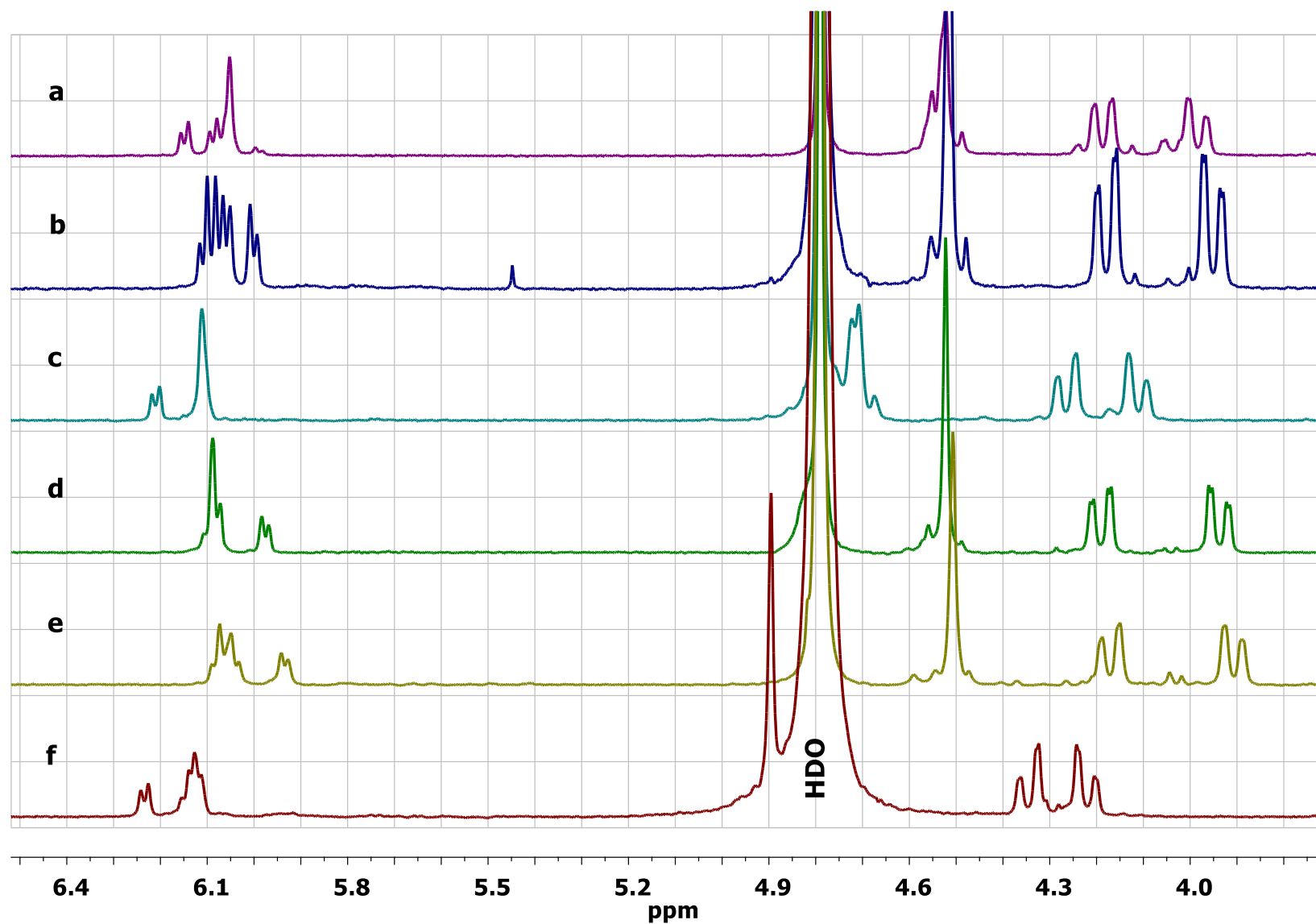


Figure S7. $^{31}\text{P}\{^1\text{H}\}$ NMR spectra of **[4]** NO_3 (a, violet line), **5** (b, blue line), **[6]** NO_3 (c, cyan line) in D_2O , **5** in D_2O + PBS solution (d, green line), **[4]** $^+/\text{D}_2\text{O}$ after Na_2CO_3 addition (e, yellow line) and after subsequent HNO_3 addition (f, red line).

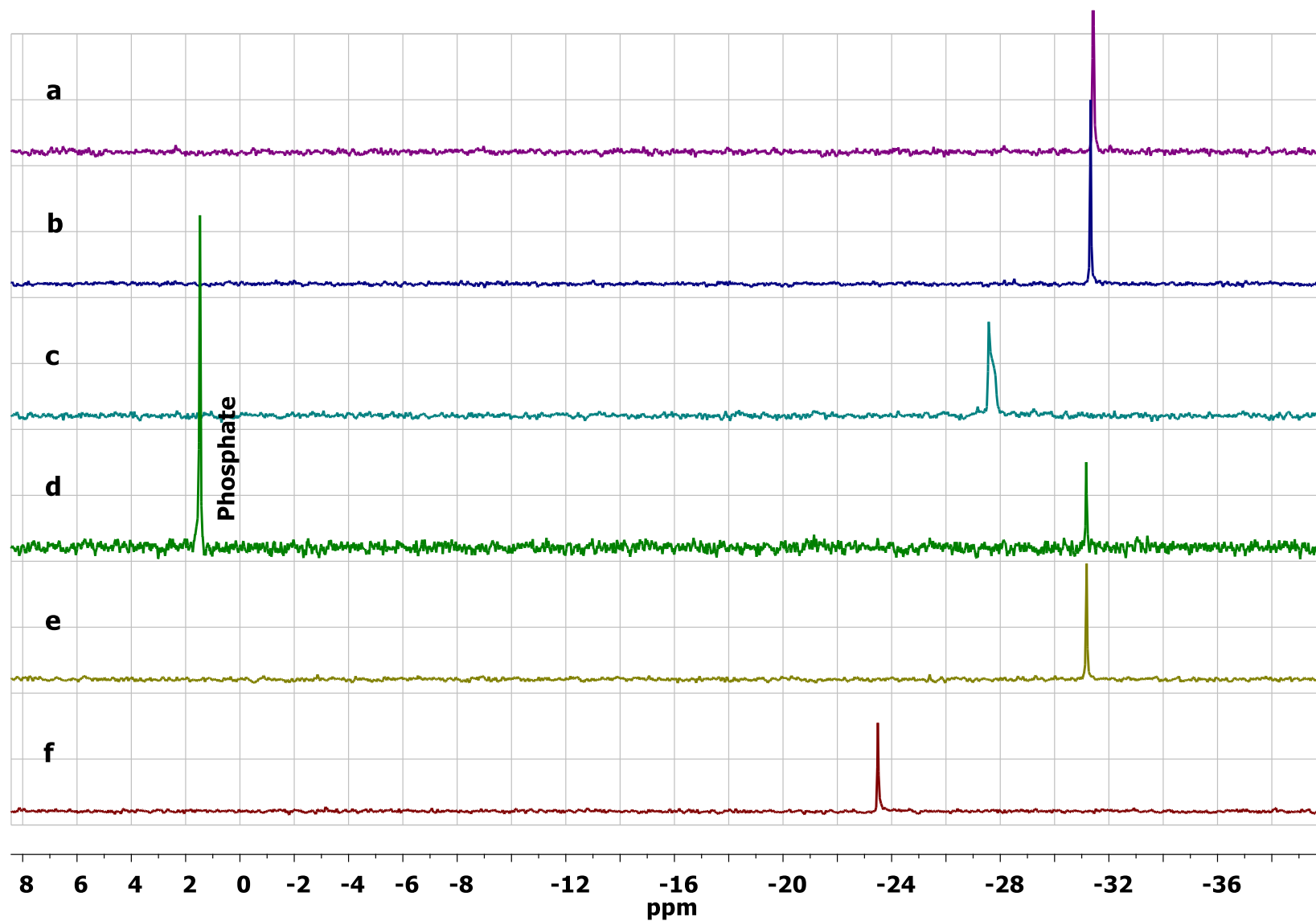


Figure S8. ^1H NMR spectra (3.80-6.50 ppm region) and $^{31}\text{P}\{^1\text{H}\}$ NMR spectra of $[\mathbf{4}]\text{NO}_3$ (a, blue line), $[\mathbf{6}]\text{NO}_3$ (b, green line) and a 1:1 mixture of $[\mathbf{4}]\text{NO}_3$ and $[\mathbf{6}]\text{NO}_3$ (c, red line) in D_2O .

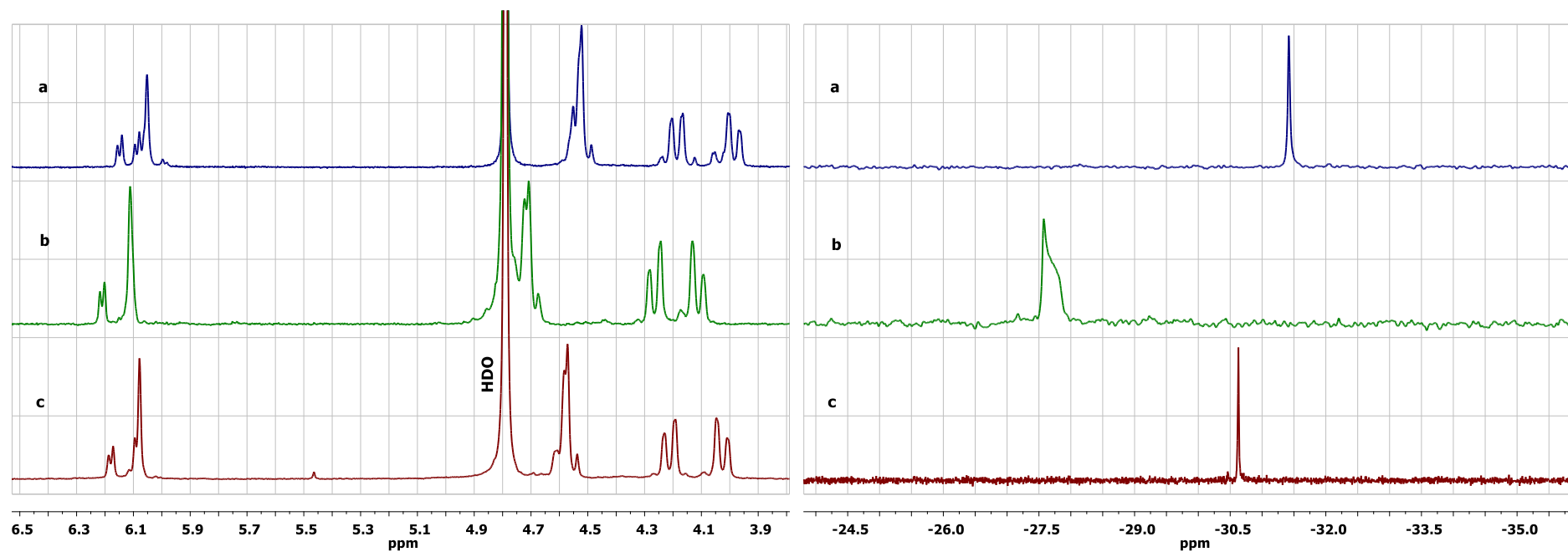


Figure S9. Solid-state IR spectrum (650-4000 cm^{-1}) of $[(\eta^6\text{-}p\text{-cymene})\text{RuCl}_2(\kappa N^{11}\text{-AcmH}_2)]$, **1A**.

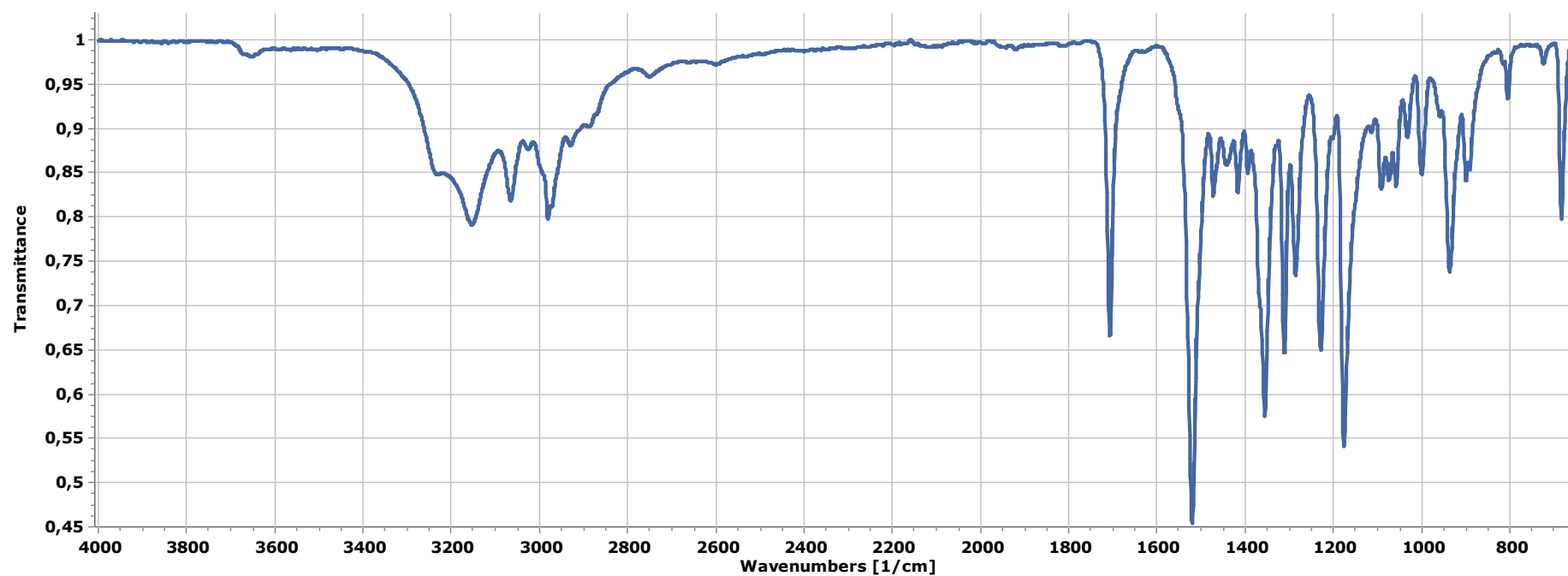


Figure S10. Solid-state IR spectrum ($650\text{-}4000\text{ cm}^{-1}$) of $[(\eta^6\text{-}p\text{-cymene})\text{RuCl}(\kappa^2\text{N}^6, \text{N}^{10}\text{-AcH})]$, **2**.

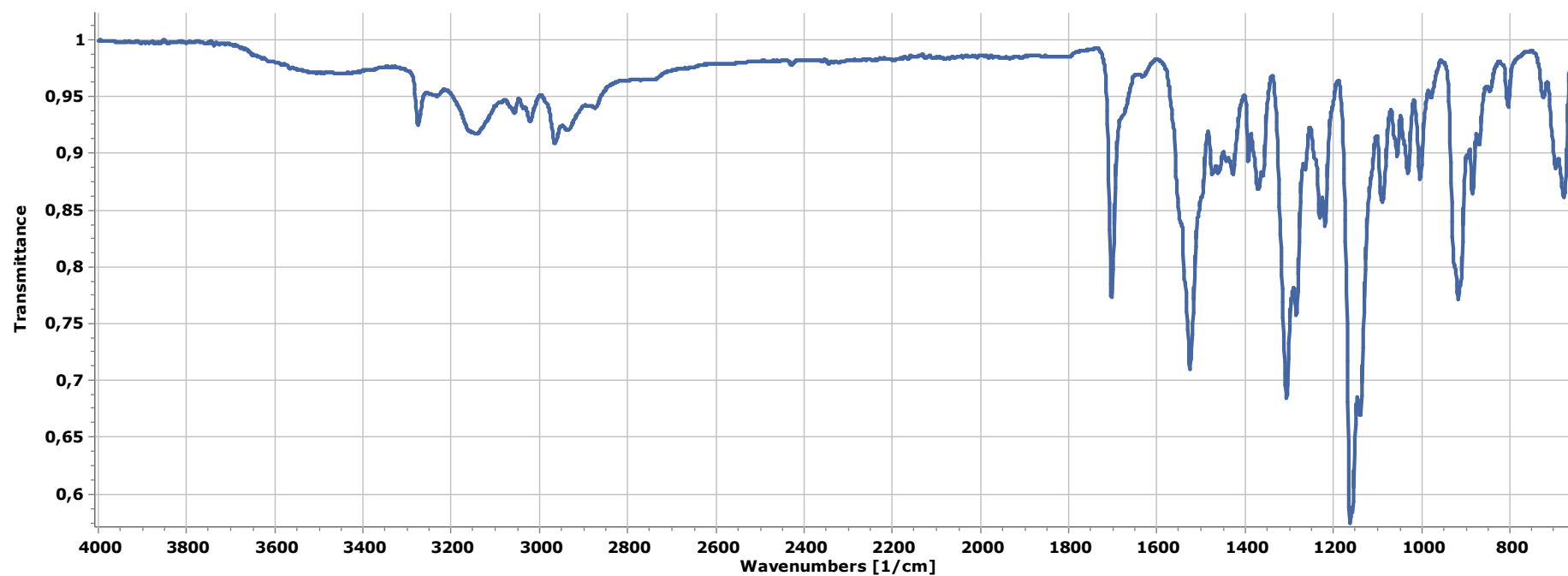


Figure S11. Solid-state IR spectrum (650-4000 cm^{-1}) of $[(\eta^6\text{-}p\text{-cymene})\text{Ru}(\kappa\text{O-NO}_3)(\kappa^2\text{N}^8, \text{N}^{10}\text{-AcmH})]$, **3**.

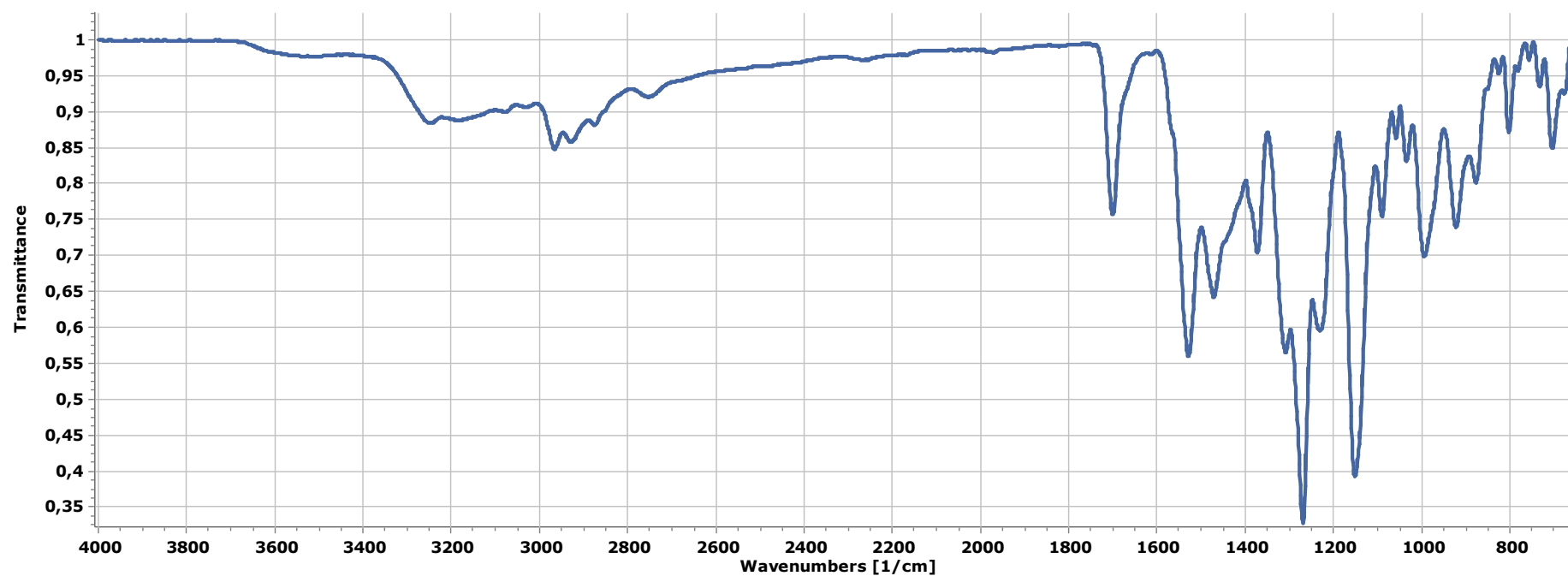


Figure S12. Solid-state IR spectrum ($650\text{--}4000\text{ cm}^{-1}$) of $[(\eta^6\text{-}p\text{-cymene})\text{Ru}(\kappa^2\text{N}^8, \text{N}^{10}\text{-AcmeH})(\kappa\text{P-pta})]\text{NO}_3$, **[4]** NO_3 .

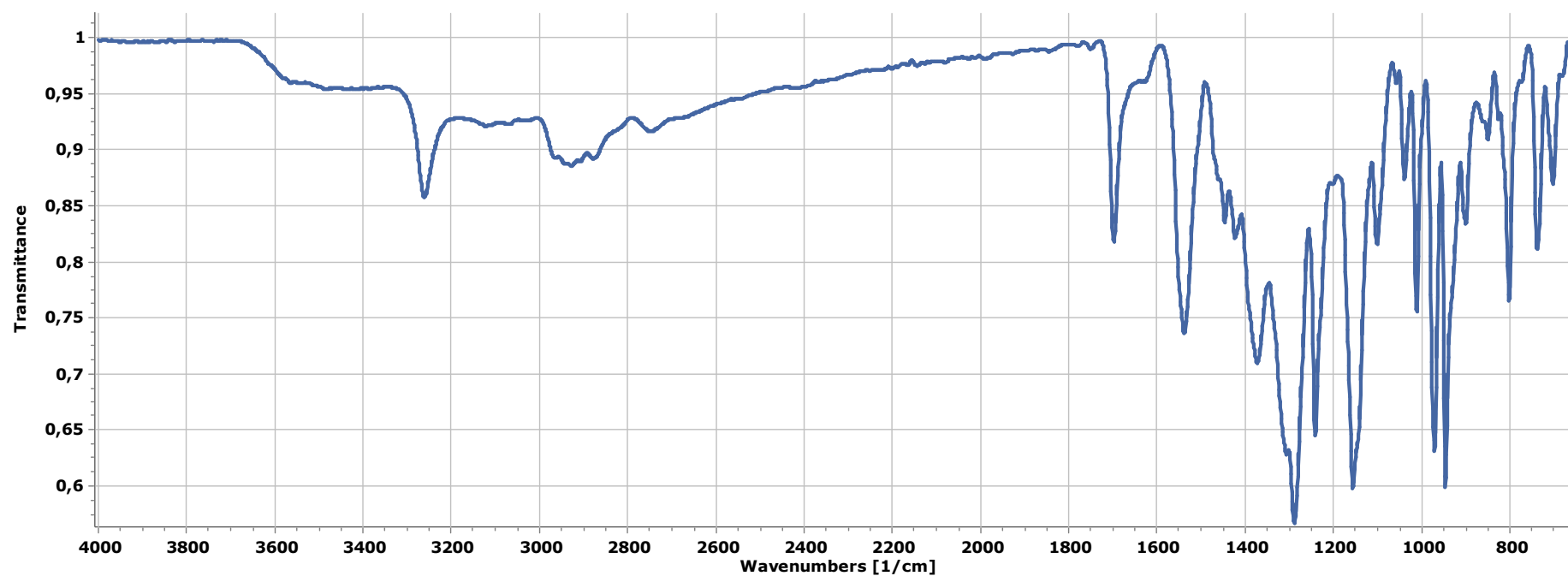


Figure S13. Solid-state IR spectrum ($650\text{-}4000\text{ cm}^{-1}$) of $[(\eta^6\text{-}p\text{-cymene})\text{Ru}(\kappa^2\text{N}^8, \text{N}^{10}\text{-AcM})(\kappa\text{P-pta})]$, **5**.

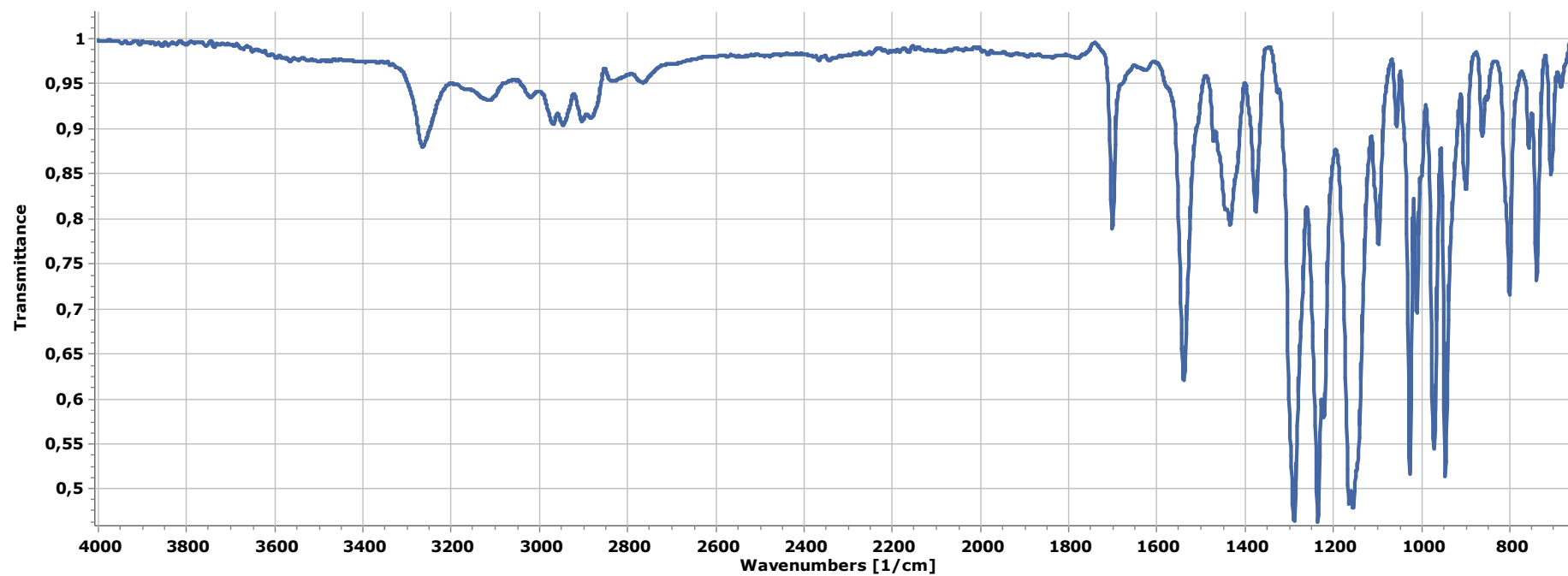


Figure S14. Solid-state IR spectrum (650-4000 cm^{-1}) of $[(\eta^6\text{-}p\text{-cymene})\text{Ru}(\kappa^2\text{N}^8, \text{N}^{10}\text{-Acn})(\kappa\text{P-ptaH})]\text{NO}_3$, **[6]** NO_3 .

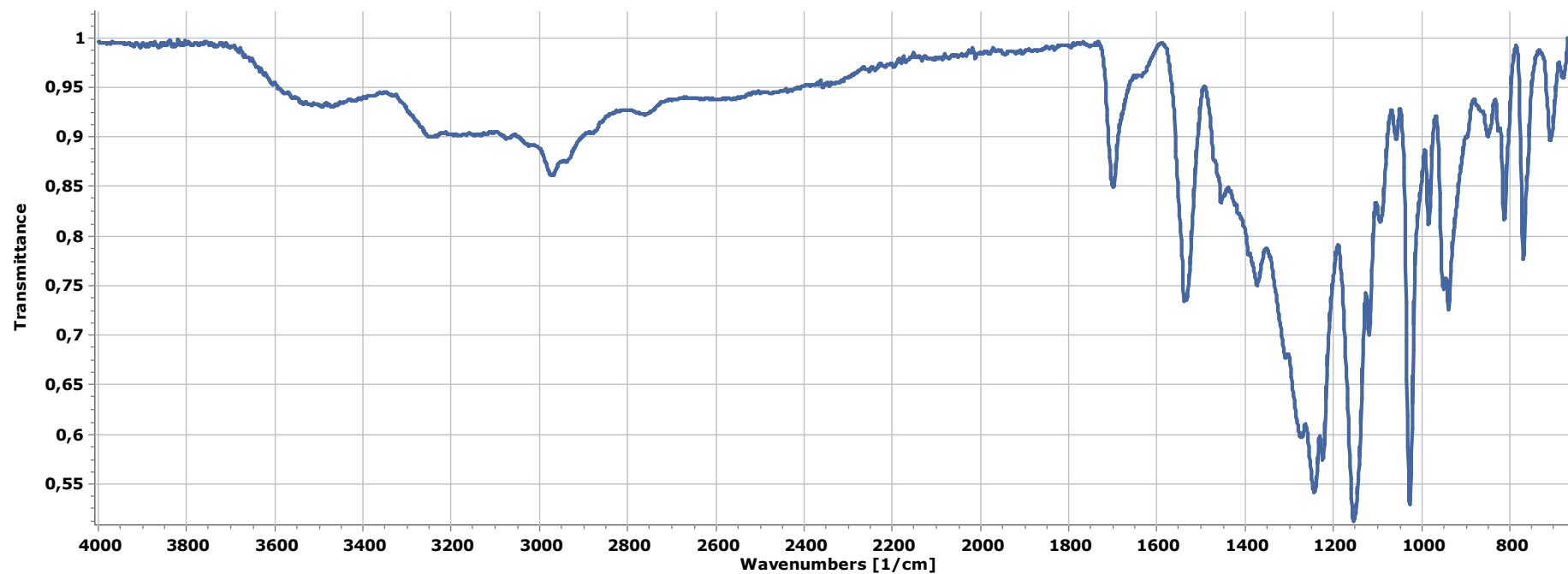


Figure S15. Solid-state IR spectrum (650-4000 cm^{-1}) of $[(\eta^6\text{-}p\text{-cymene})\text{Ru}(\kappa^2\text{N}^6, \text{N}^{10}\text{-Acm})(\kappa\text{P-ptaH})][\text{TsO}]$, **[6]** $[\text{TsO}]$.

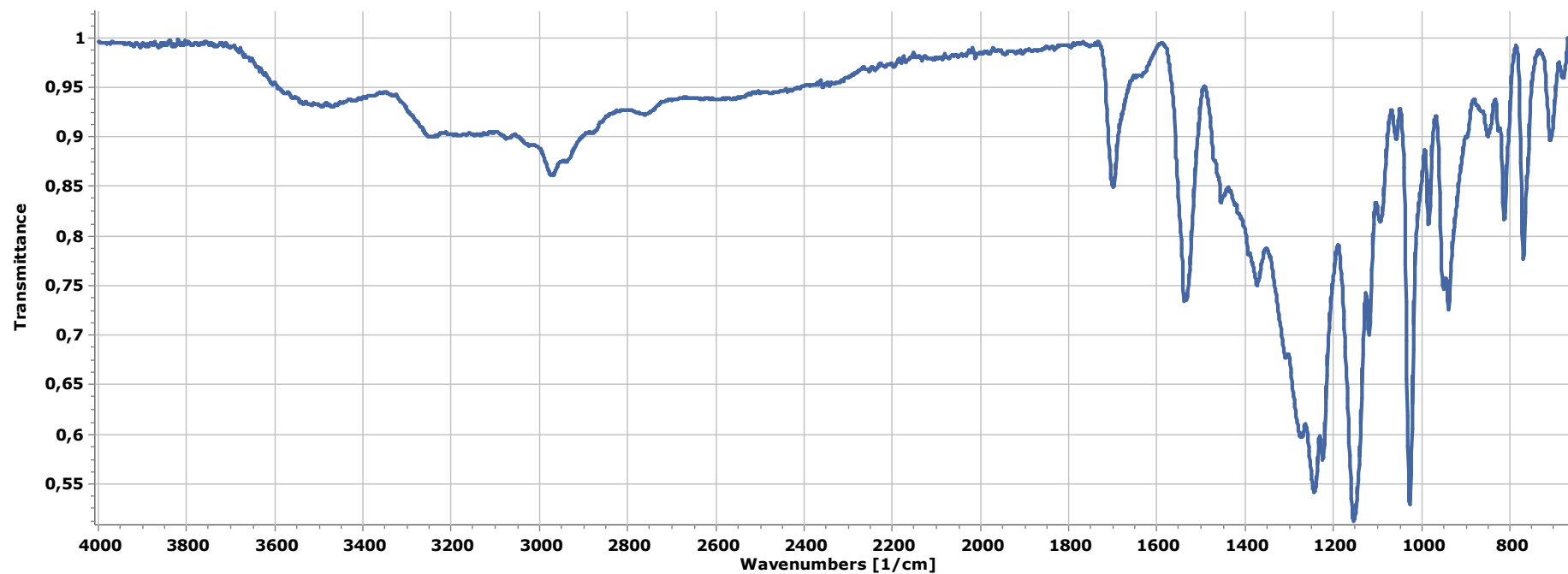


Figure S16. ^1H NMR spectrum (401 MHz, acetone- d_6) of $[(\eta^6\text{-}p\text{-cymene})\text{RuCl}_2(\kappa N^1\text{-AcmH}_2)]$, **1A**.

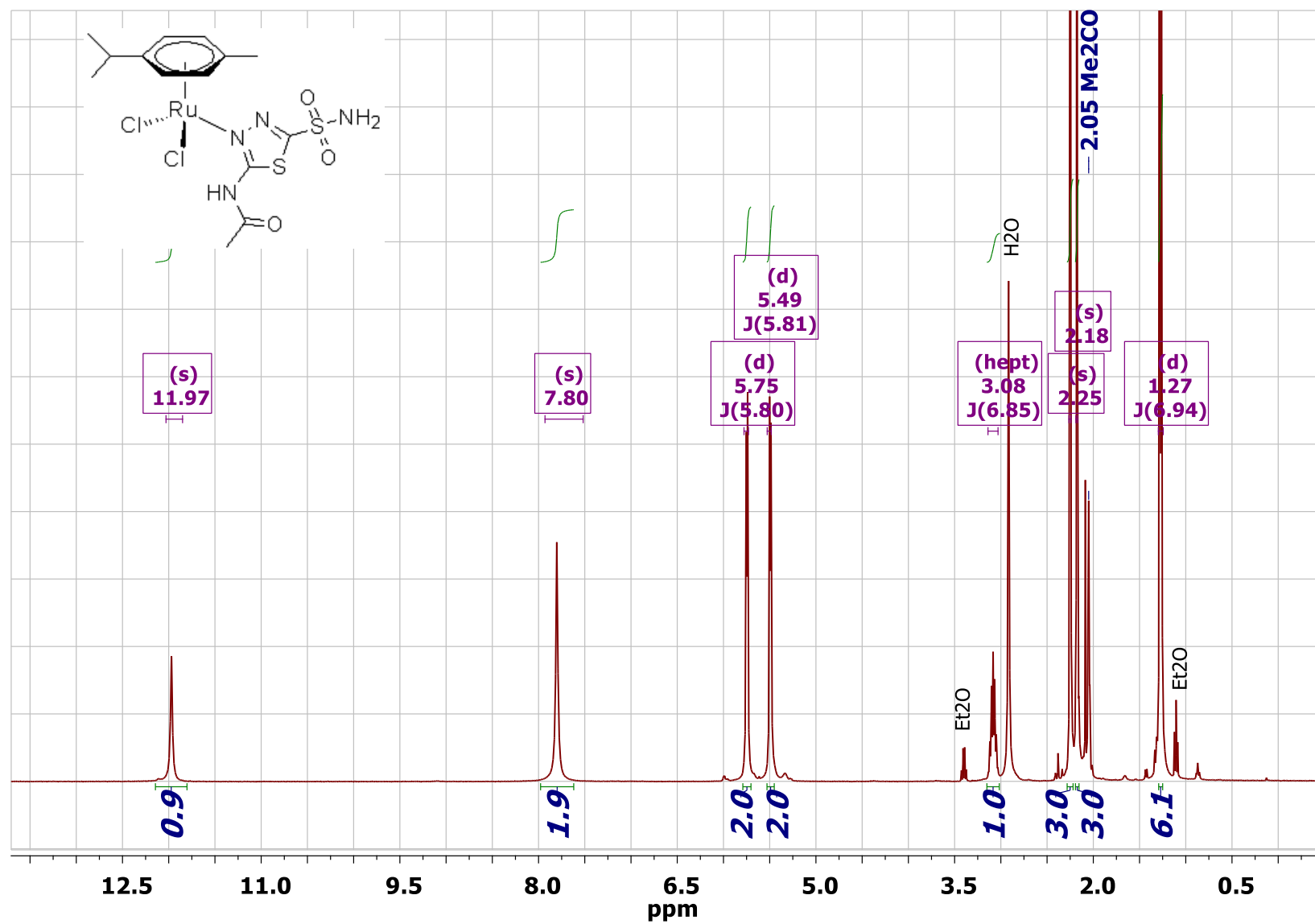


Figure S17. $^{13}\text{C}\{^1\text{H}\}$ NMR spectrum (101 MHz, acetone- d_6) of $[(\eta^6\text{-}p\text{-cymene})\text{RuCl}_2(\kappa\text{N}^1\text{-AcmH}_2)]$, **1A**.

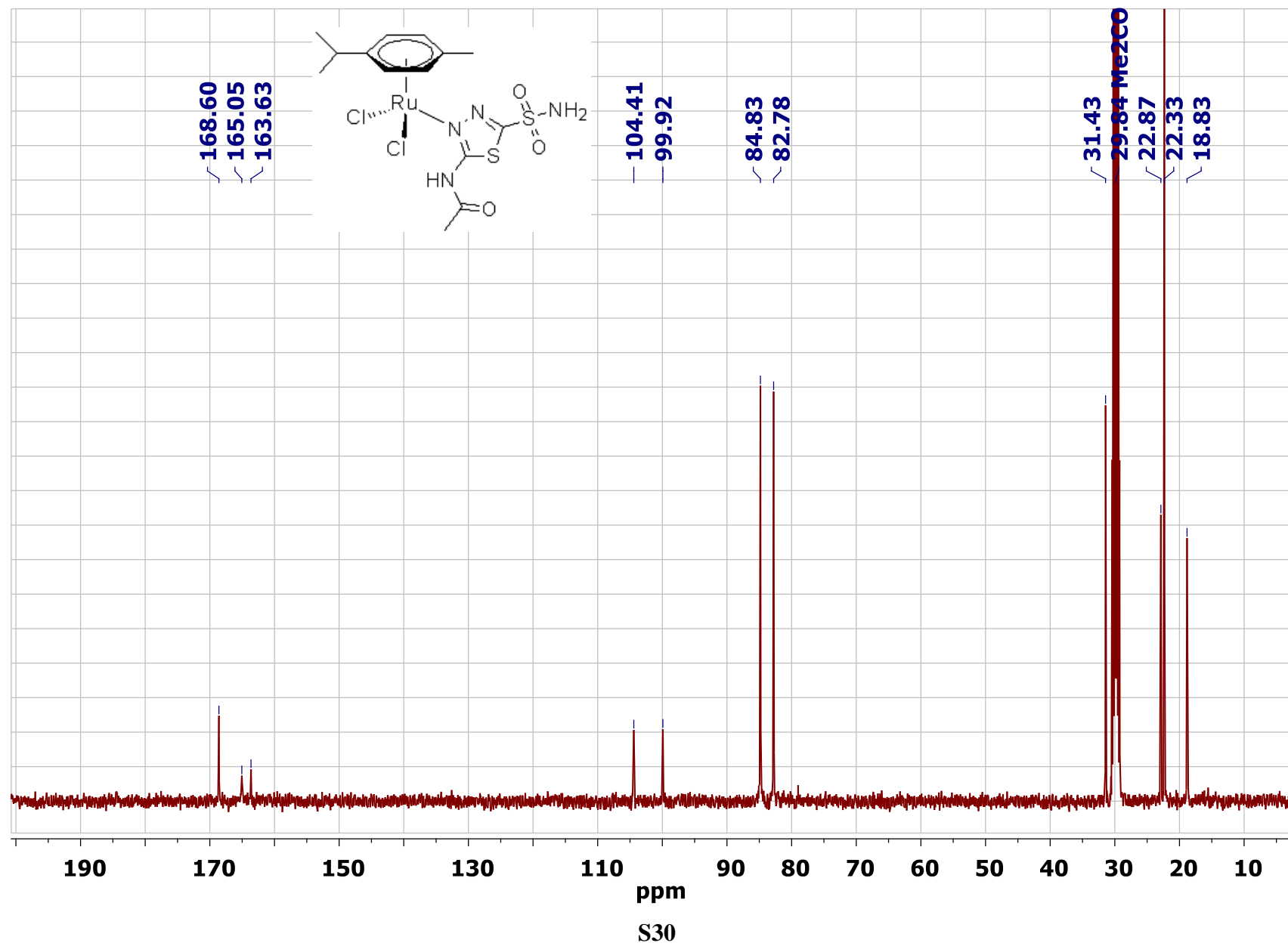


Figure S18. ^1H NMR spectrum (401 MHz, CD_3NO_2) of $[(\eta^6\text{-}p\text{-cymene})\text{RuCl}(\kappa^2\text{N}^8, \text{N}^{10}\text{-AcmH})]$, **2**. Inset shows the acetamide NH resonance.

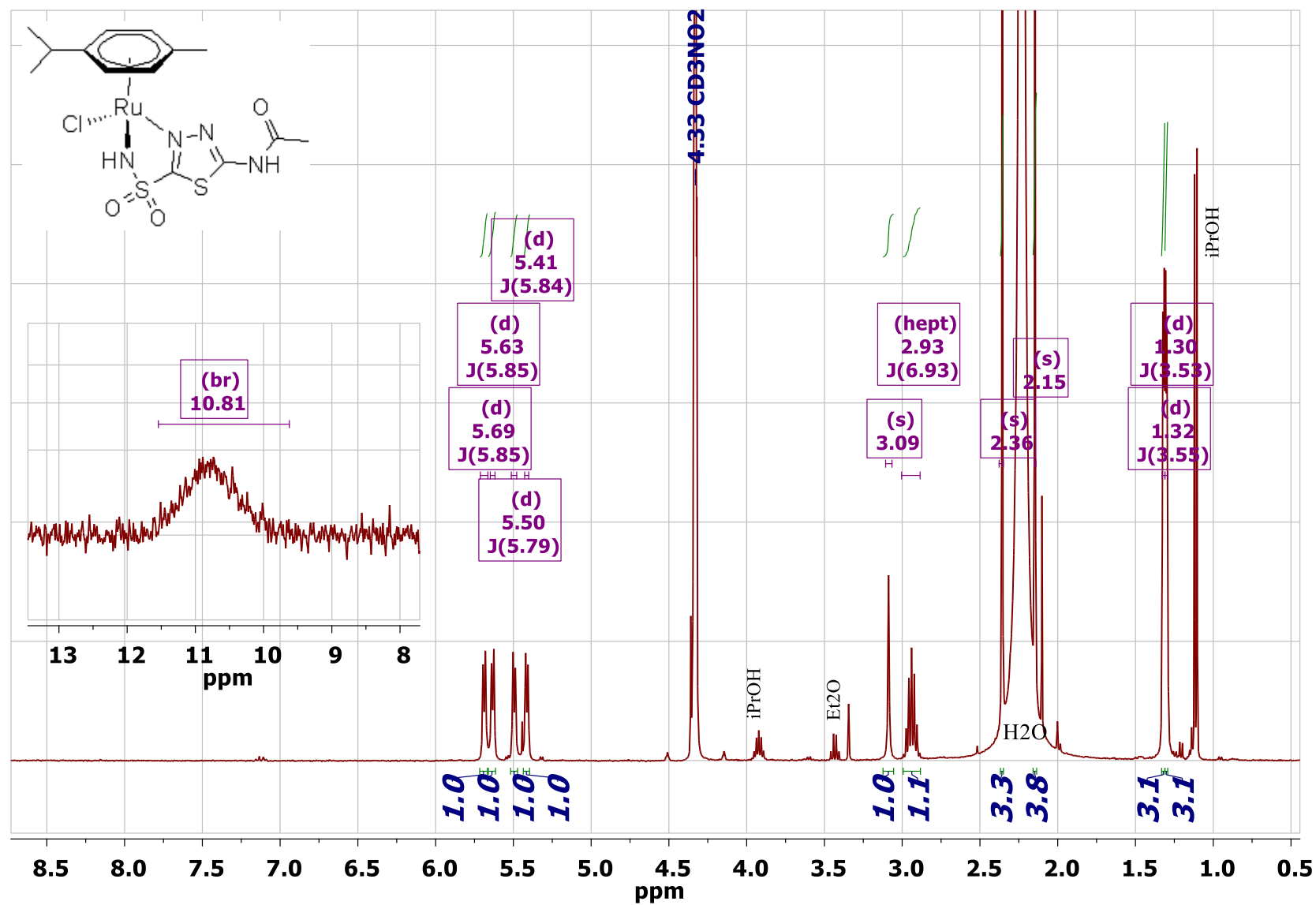


Figure S19. $^{13}\text{C}\{^1\text{H}\}$ NMR spectrum (101 MHz, CD_3NO_2) of $[(\eta^6\text{-}p\text{-cymene})\text{RuCl}(\kappa^2 N^6, N^{10}\text{-Acmh})]$, **2**.

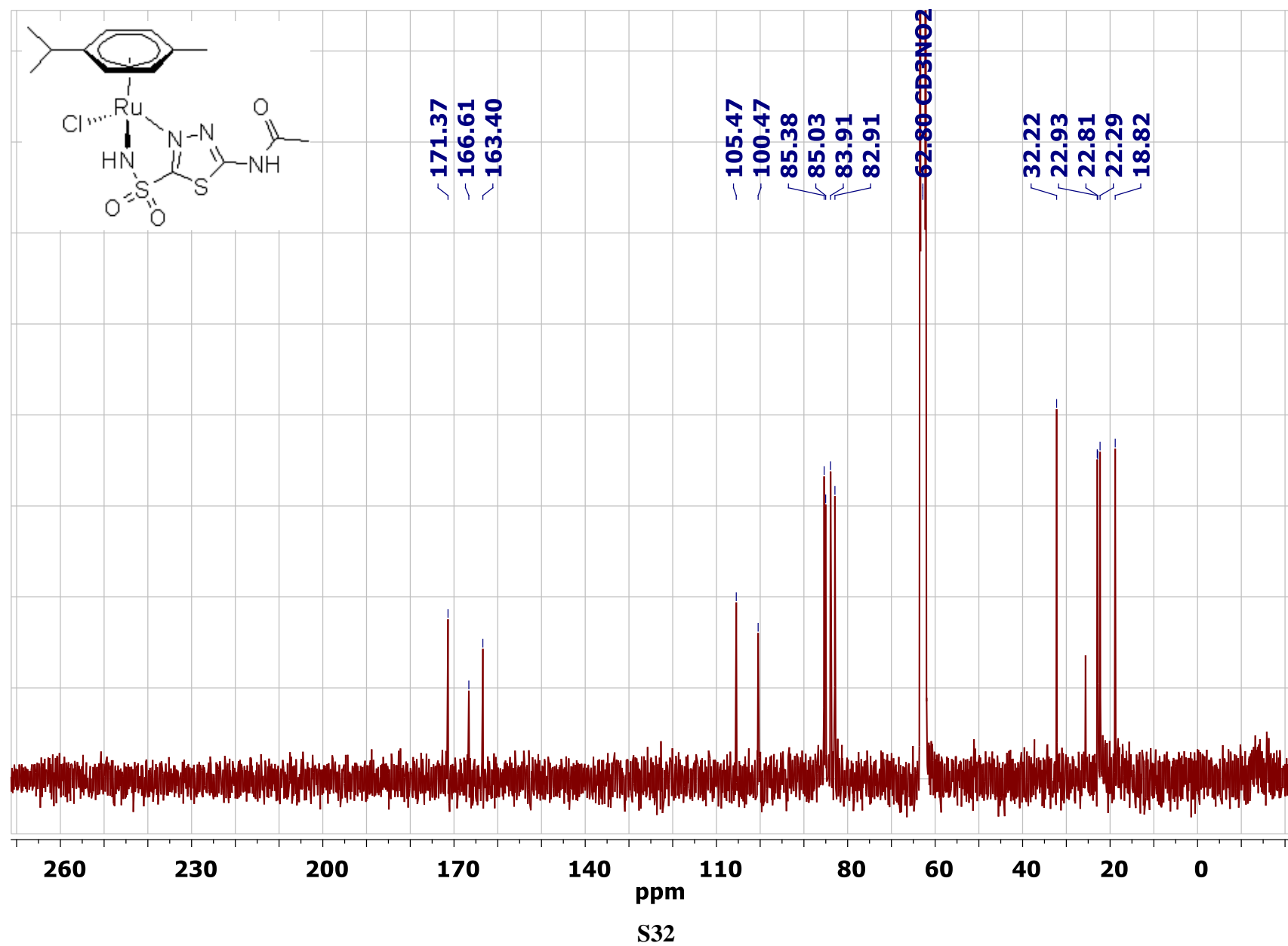


Figure S20. ^1H NMR spectrum (401 MHz, CD_3CN) of $[(\eta^6\text{-}p\text{-cymene})\text{Ru}(\kappa\text{O-NO}_3)(\kappa^2\text{N}^6, \text{N}^{10}\text{-AcmH})]$, **3**. Inset shows the acetamide NH resonance.

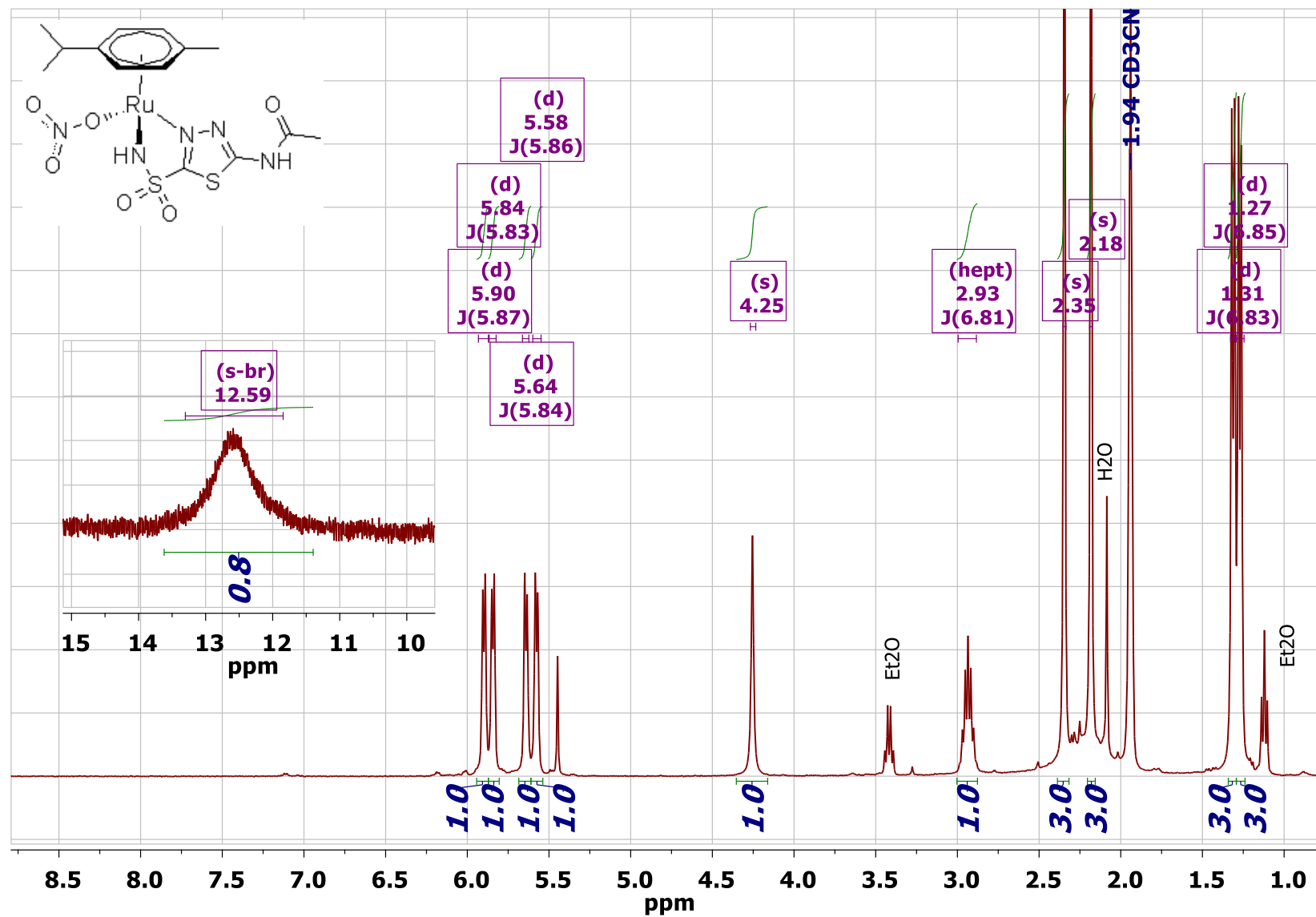


Figure S21. $^{13}\text{C}\{^1\text{H}\}$ NMR spectrum (101 MHz, CD_3CN) of $[(\eta^6\text{-}p\text{-cymene})\text{Ru}(\kappa\text{O-NO}_3)(\kappa^2\text{N}^8, \text{N}^{10}\text{-AcmH})]$, **3**.

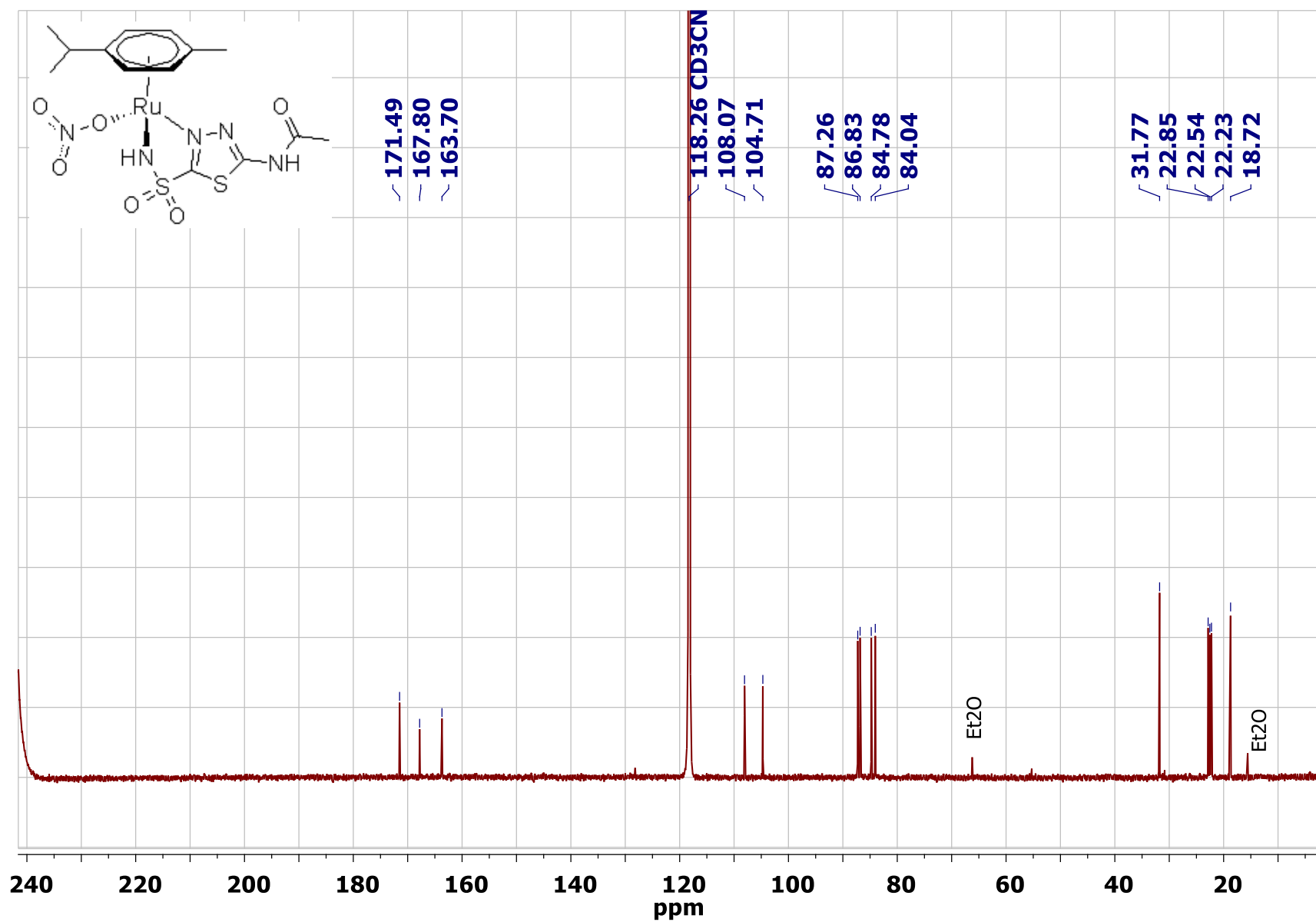


Figure S22. ^{14}N NMR spectrum (29 MHz, CD_3CN) of $[(\eta^6\text{-}p\text{-cymene})\text{Ru}(\kappa\text{O-NO}_3)(\kappa^2\text{N}^8, \text{N}^{10}\text{-AcmH})]$, **3**.

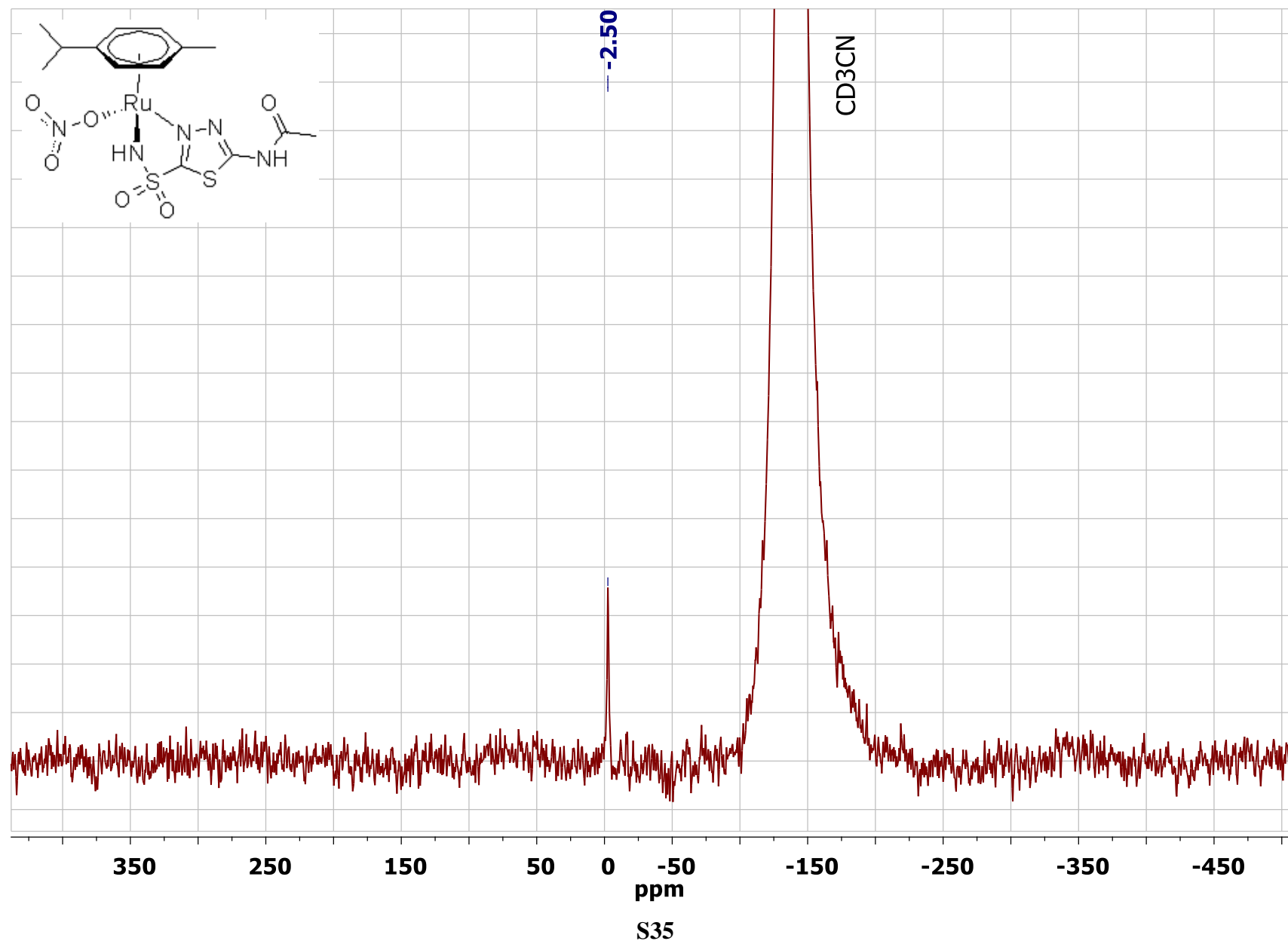


Figure S23. ^1H NMR spectrum (401 MHz, CD_3OD) of $[(\eta^6\text{-}p\text{-cymene})\text{Ru}(\kappa^2 N^6, N^{10}\text{-AcmH})(\kappa P\text{-pta})]\text{NO}_3$, **[4]** NO_3 .

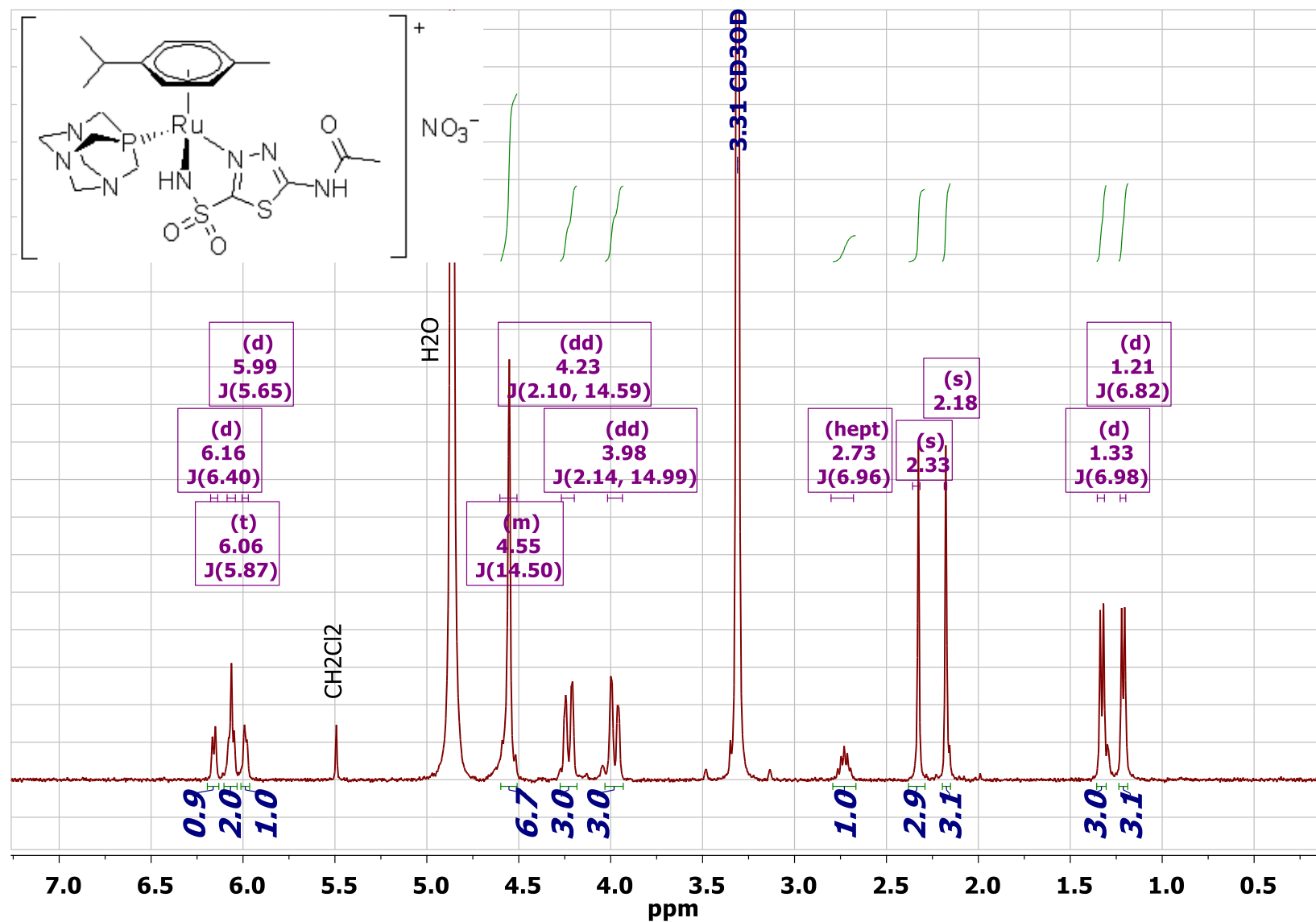


Figure S24. $^{13}\text{C}\{^1\text{H}\}$ NMR spectrum (101 MHz, CD_3OD) of $[(\eta^6\text{-}p\text{-cymene})\text{Ru}(\kappa^2\text{N}^6, \text{N}^{10}\text{-Acmh})(\kappa\text{P-pta})]\text{NO}_3$, **[4]** NO_3 .

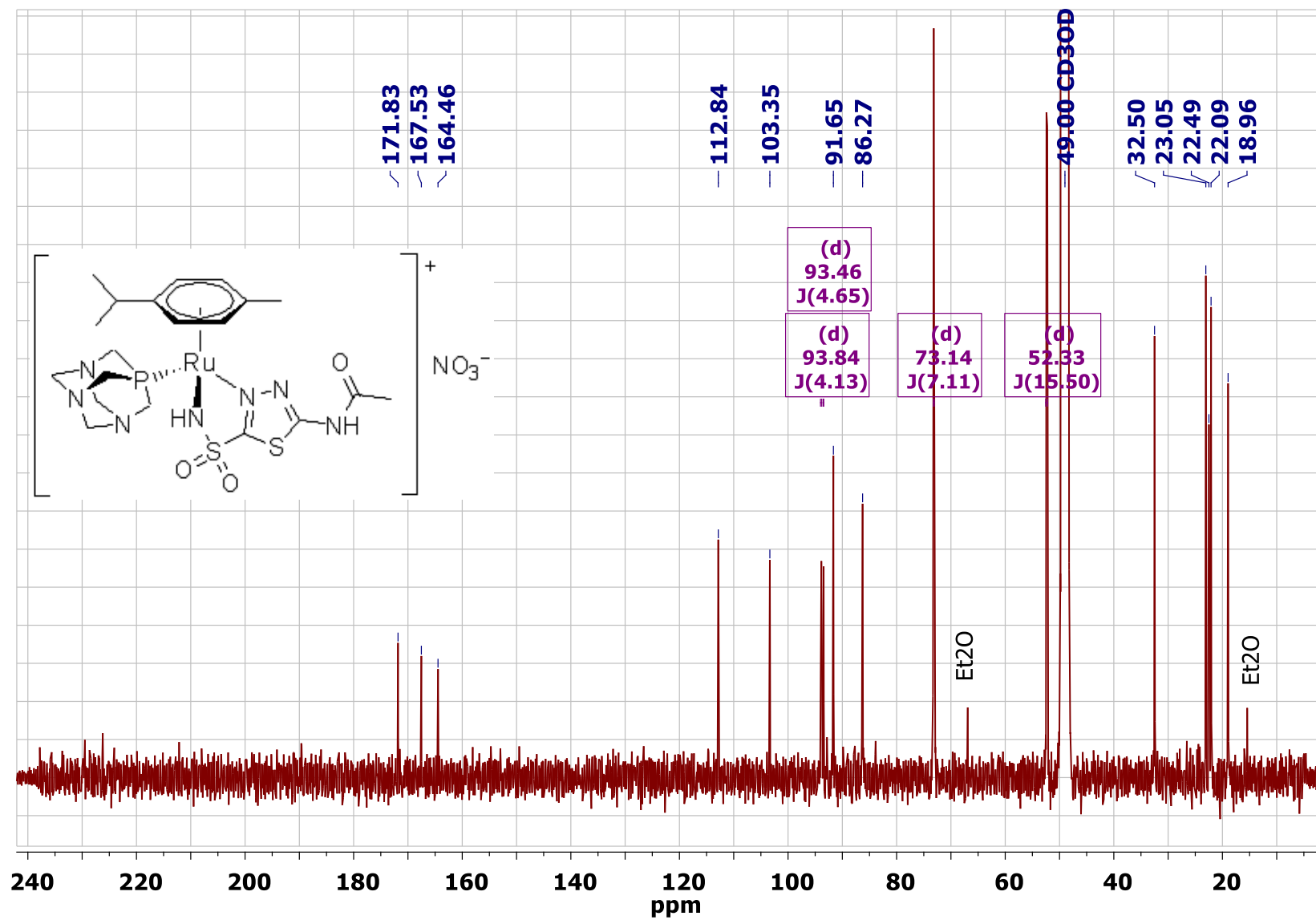


Figure S25. ^{14}N NMR spectrum (29 MHz, CD_3OD) of $[(\eta^6\text{-}p\text{-cymene})\text{Ru}(\kappa^2 N^6, N^{10}\text{-Acmh})(\kappa P\text{-pta})]\text{NO}_3$, **[4]** NO_3 .

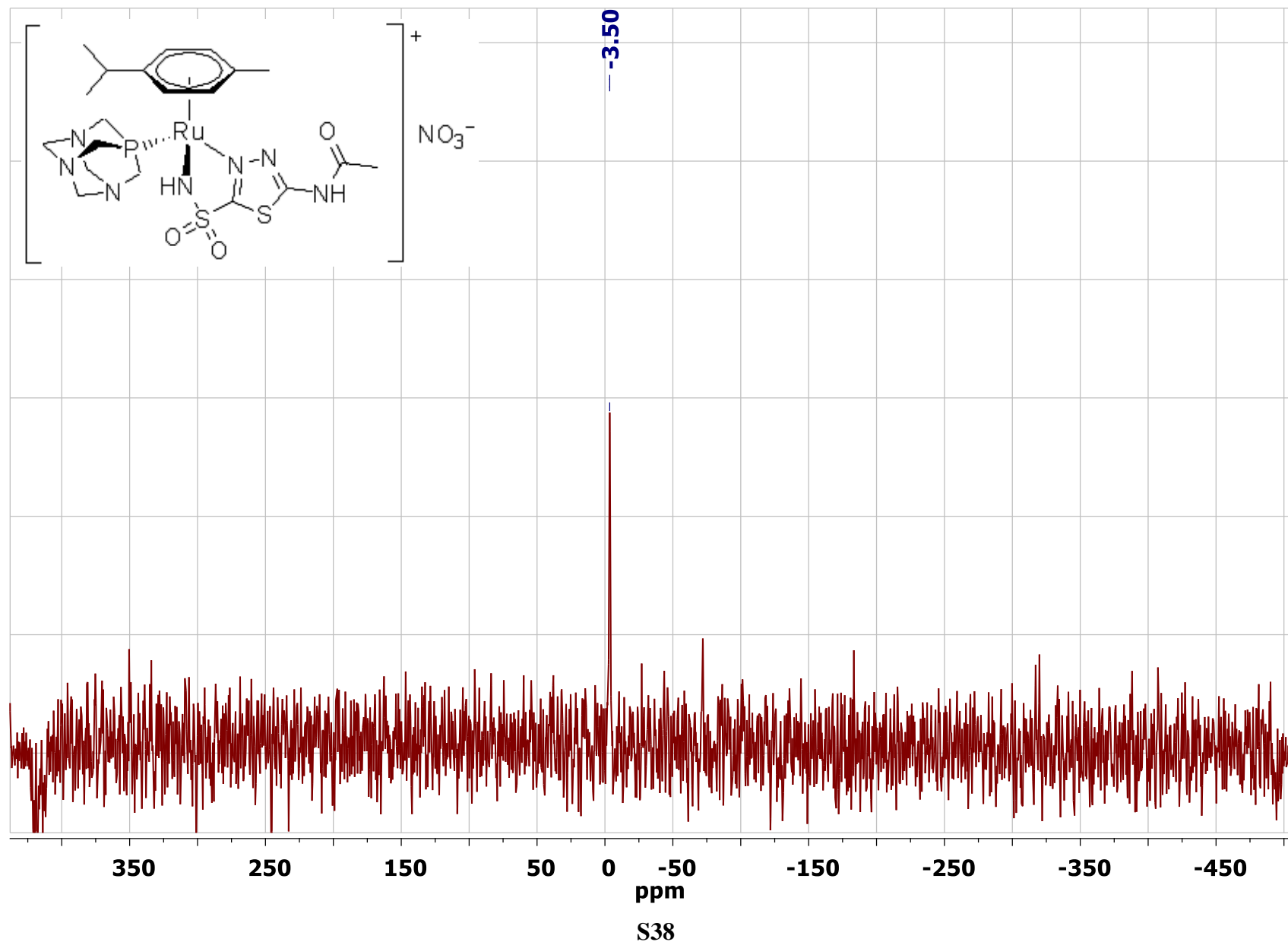


Figure S26. $^{31}\text{P}\{^1\text{H}\}$ NMR spectrum (162 MHz, CD_3OD) of $[(\eta^6\text{-}p\text{-cymene})\text{Ru}(\kappa^2\text{N}^8, \text{N}^{10}\text{-AcmH})(\kappa\text{P-pta})]\text{NO}_3$, **[4]** NO_3 .

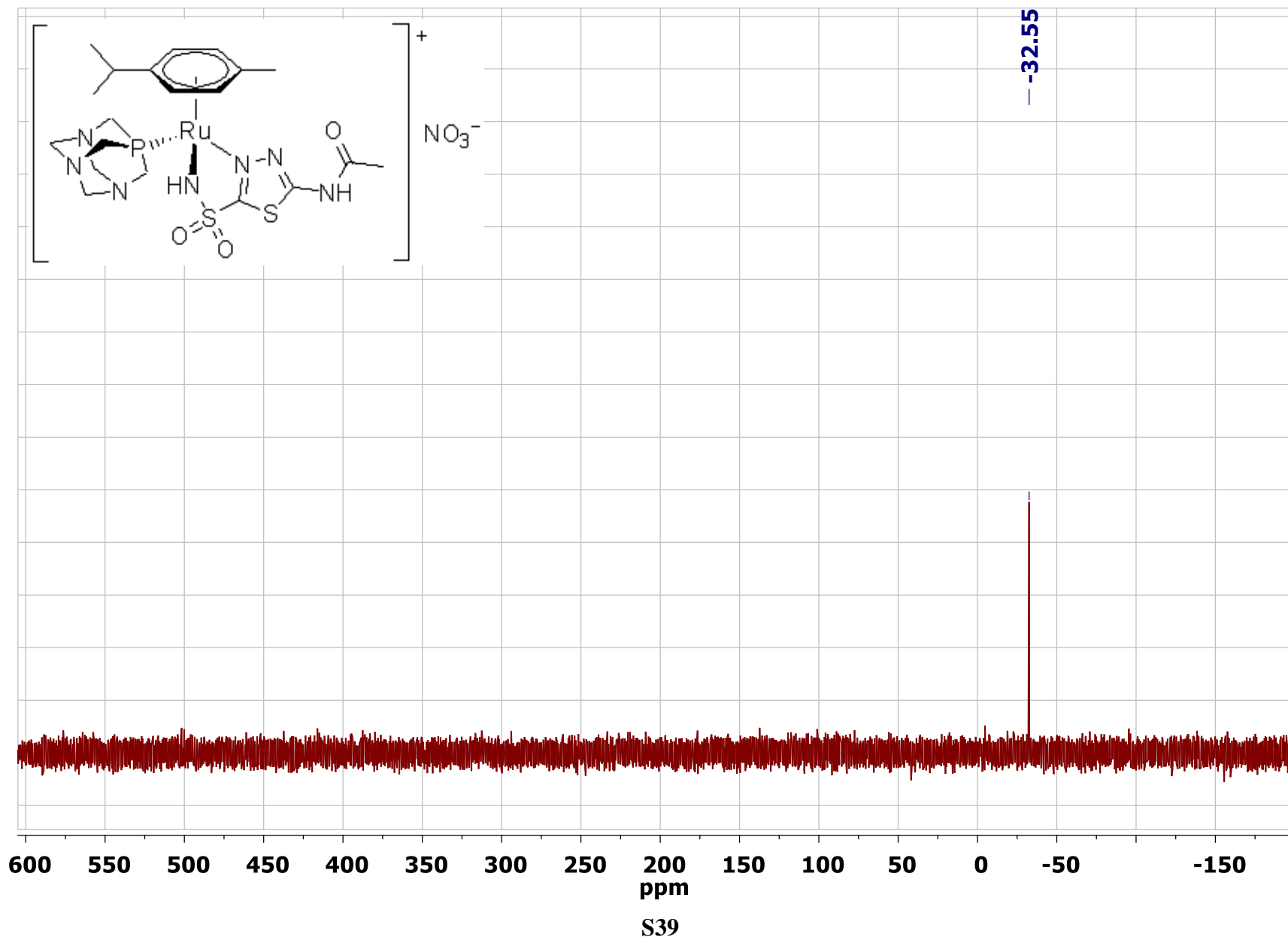


Figure S27. ^1H NMR spectrum (401 MHz, CD_3OD) of $[(\eta^6\text{-}p\text{-cymene})\text{Ru}(\kappa^2\text{N}^6, \text{N}^{10}\text{-Acm})(\kappa\text{P-pta})]$, **5**.

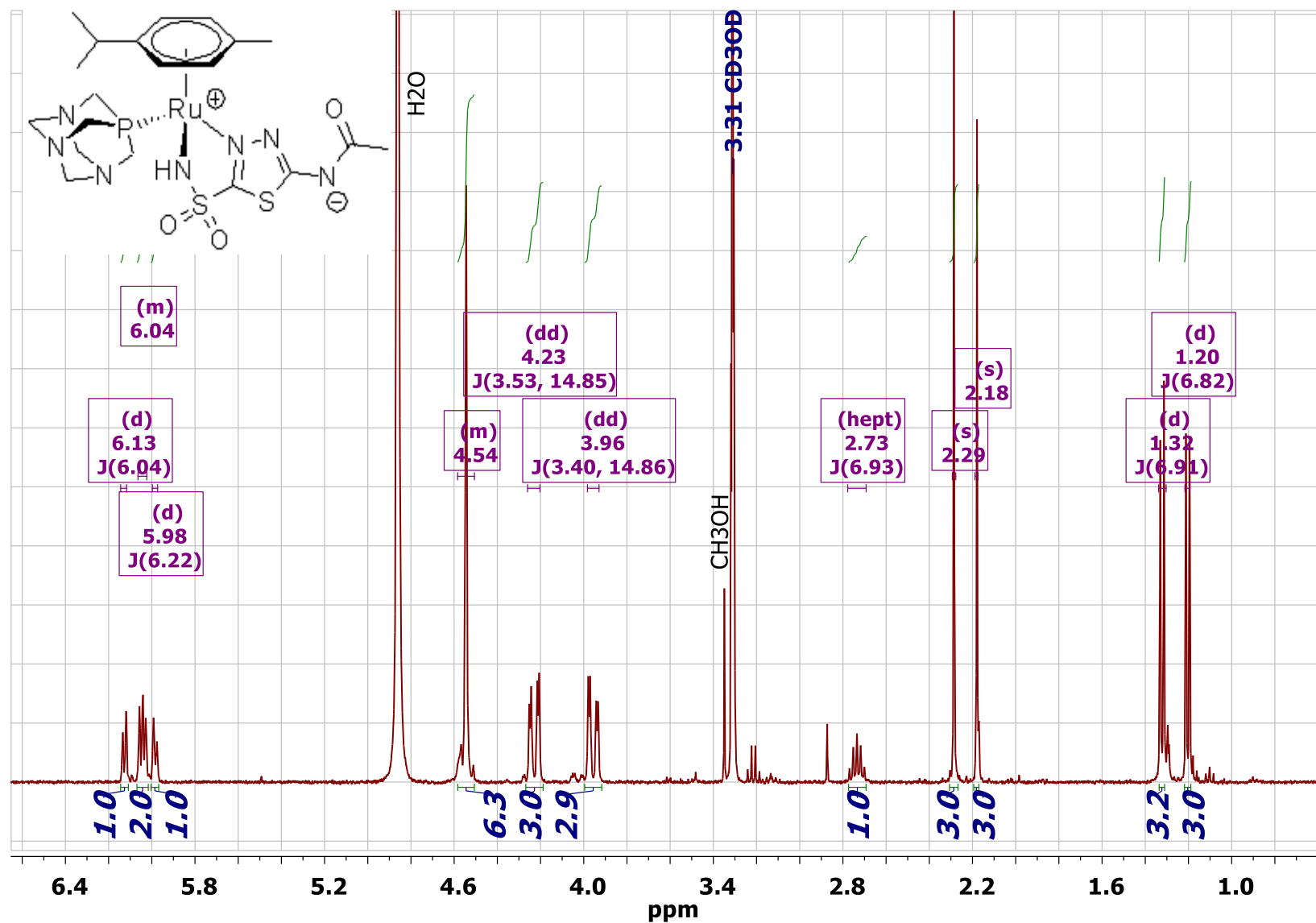


Figure S28. $^{13}\text{C}\{^1\text{H}\}$ NMR spectrum (101 MHz, CD_3OD) of $[(\eta^6\text{-}p\text{-cymene})\text{Ru}(\kappa^2\text{N}^6, \text{N}^{10}\text{-Acm})(\kappa\text{P-pta})]$, **5**. Signals for the C=N atoms of the 1,3,5-thiadiazole ring and the C=O atom were not detected; the latter was identified by the gs-HMBC experiment.

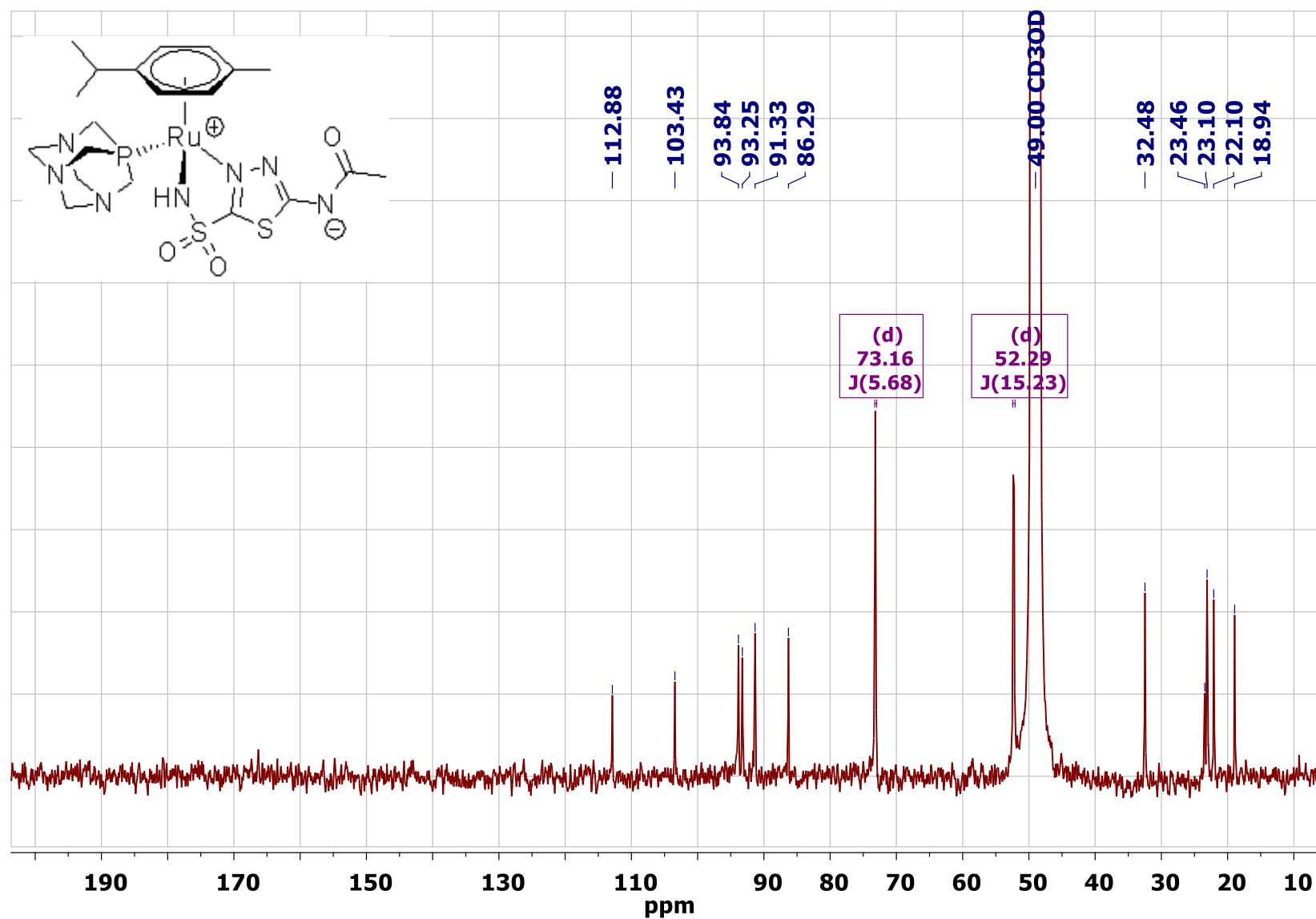


Figure S29. $^{31}\text{P}\{^1\text{H}\}$ NMR spectrum (162 MHz, CD_3OD) of $[(\eta^6\text{-}p\text{-cymene})\text{Ru}(\kappa^2\text{N}^8, \text{N}^{10}\text{-Acm})(\kappa\text{P-pta})]$, **5**.

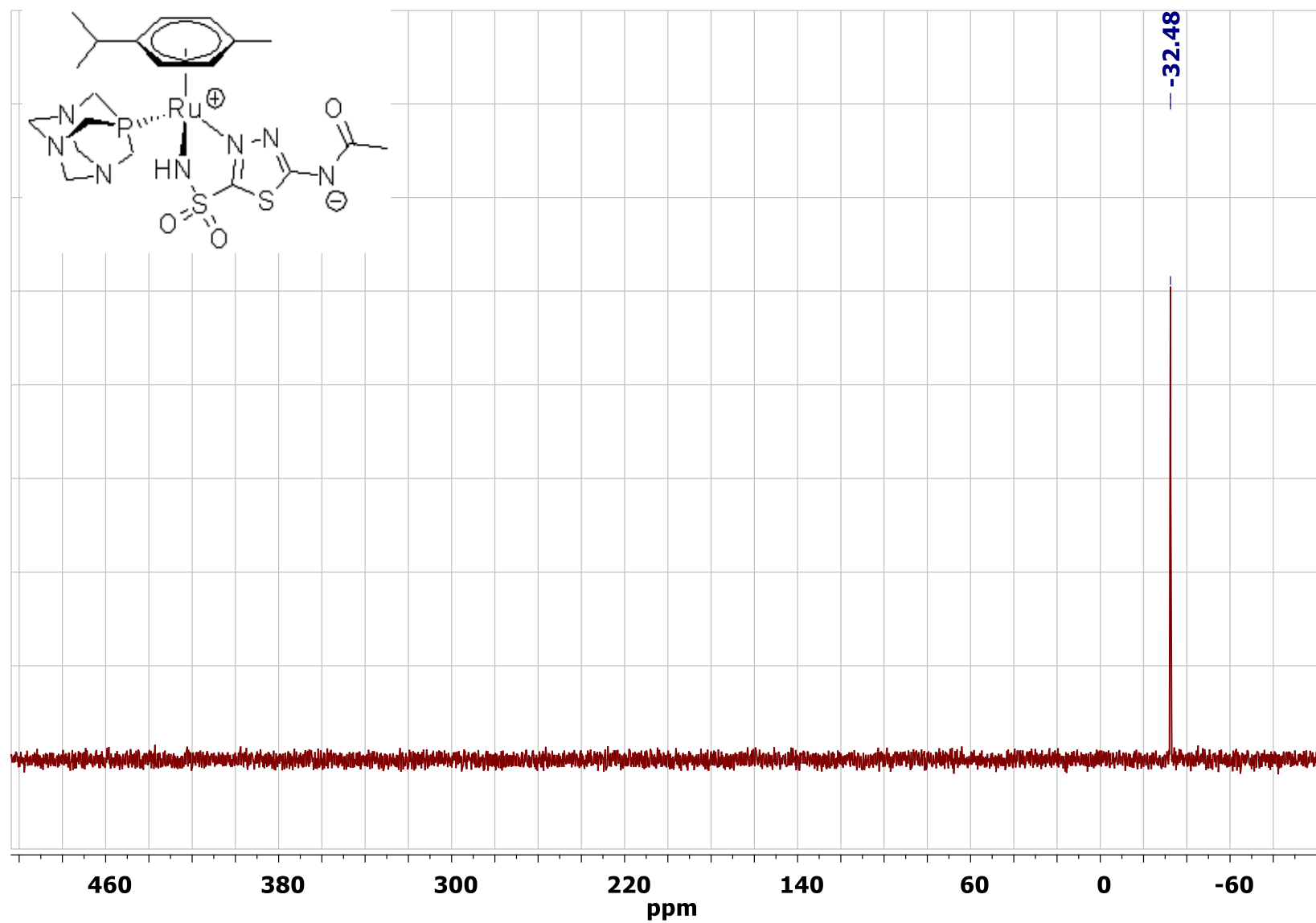


Figure S30. ^1H NMR spectrum (401 MHz, CD_3OD) of $[(\eta^6\text{-}p\text{-cymene})\text{Ru}(\kappa^2\text{N}^6, \text{N}^{10}\text{-Acm})(\kappa\text{P-ptaH})]\text{NO}_3$, $[\mathbf{6}]\text{NO}_3$ ($\text{H}_2\text{O}/[\mathbf{6}]^+$ mol. ratio ≈ 13 mol. ratio 14).

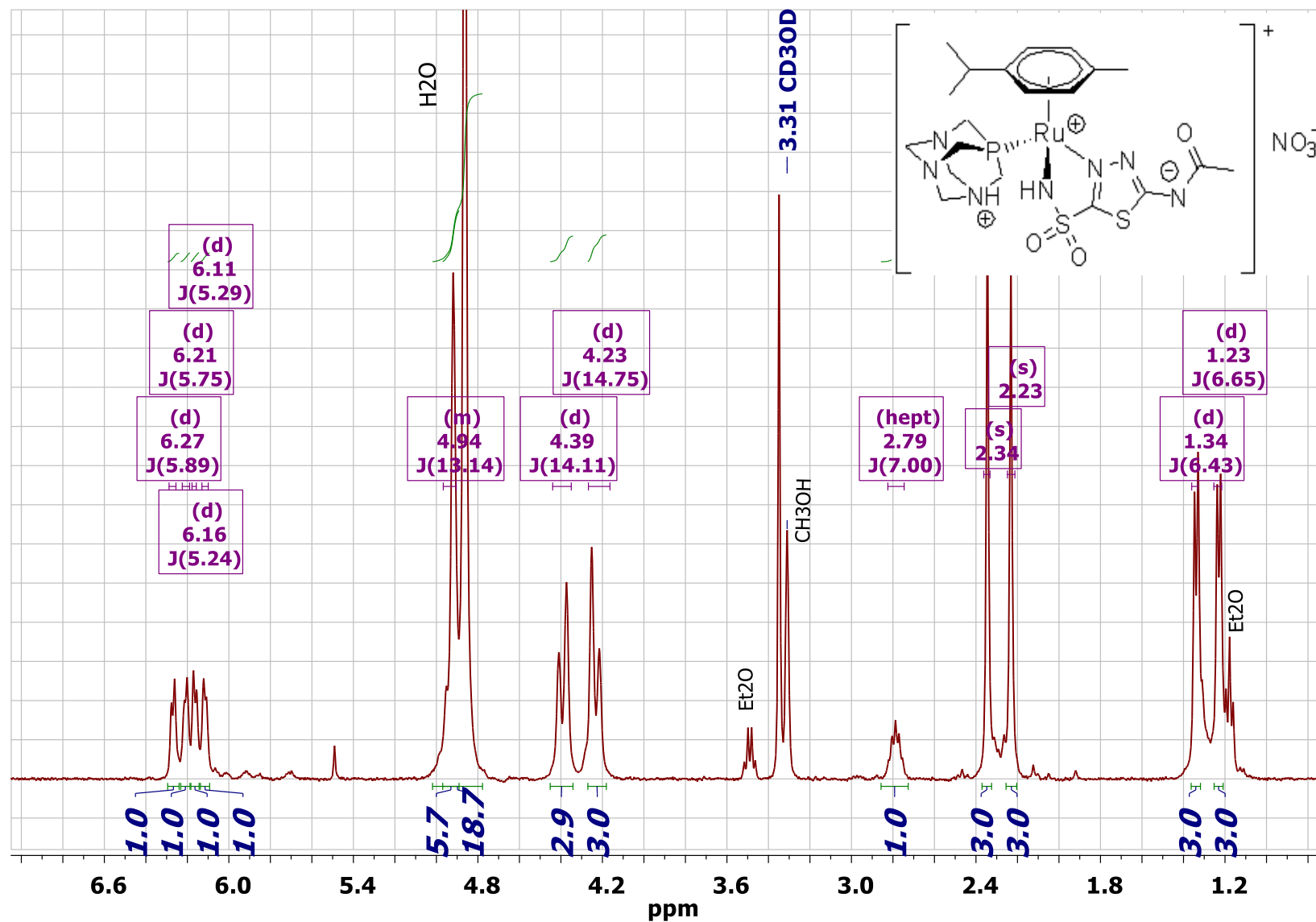


Figure S31. $^{13}\text{C}\{^1\text{H}\}$ NMR spectrum (101 MHz, CD_3OD) of $[(\eta^6\text{-}p\text{-cymene})\text{Ru}(\kappa^2\text{N}^6, \text{N}^{10}\text{-Acm})(\kappa\text{P-ptaH})]\text{NO}_3$, $[\text{6}]\text{NO}_3$ ($\text{H}_2\text{O}/[\text{6}]^+$ mol. ratio ≈ 13 mol. ratio 14).

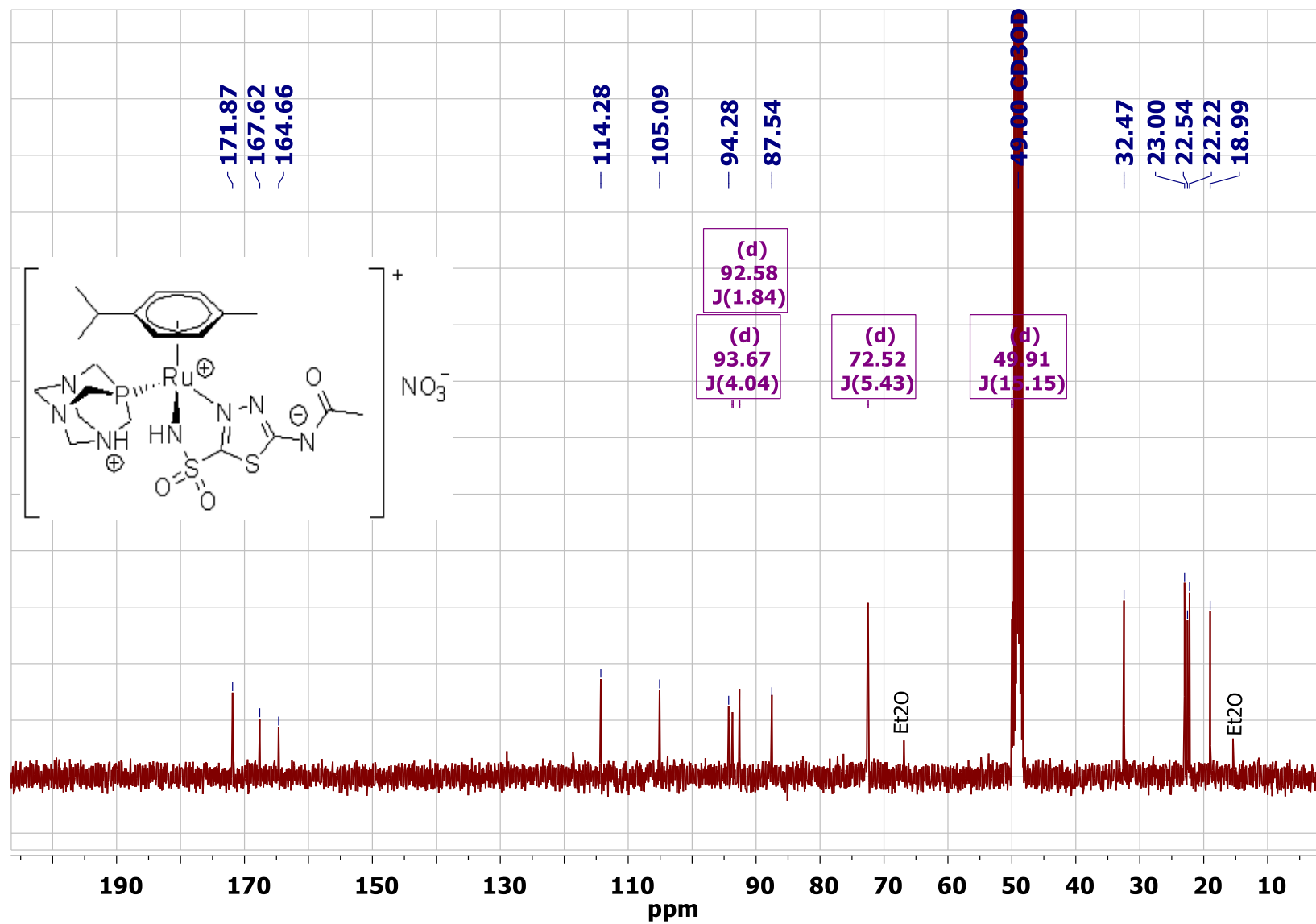


Figure S32. ^{14}N NMR spectrum (29 MHz, CD_3OD) of $[(\eta^6\text{-}p\text{-cymene})\text{Ru}(\kappa^2\text{N}^6, \text{N}^{10}\text{-Acm})(\kappa\text{P-ptaH})]\text{NO}_3$, $[\mathbf{6}]\text{NO}_3$ ($\text{H}_2\text{O}/[\mathbf{6}]^+$ mol. ratio ≈ 13 mol. ratio 14).

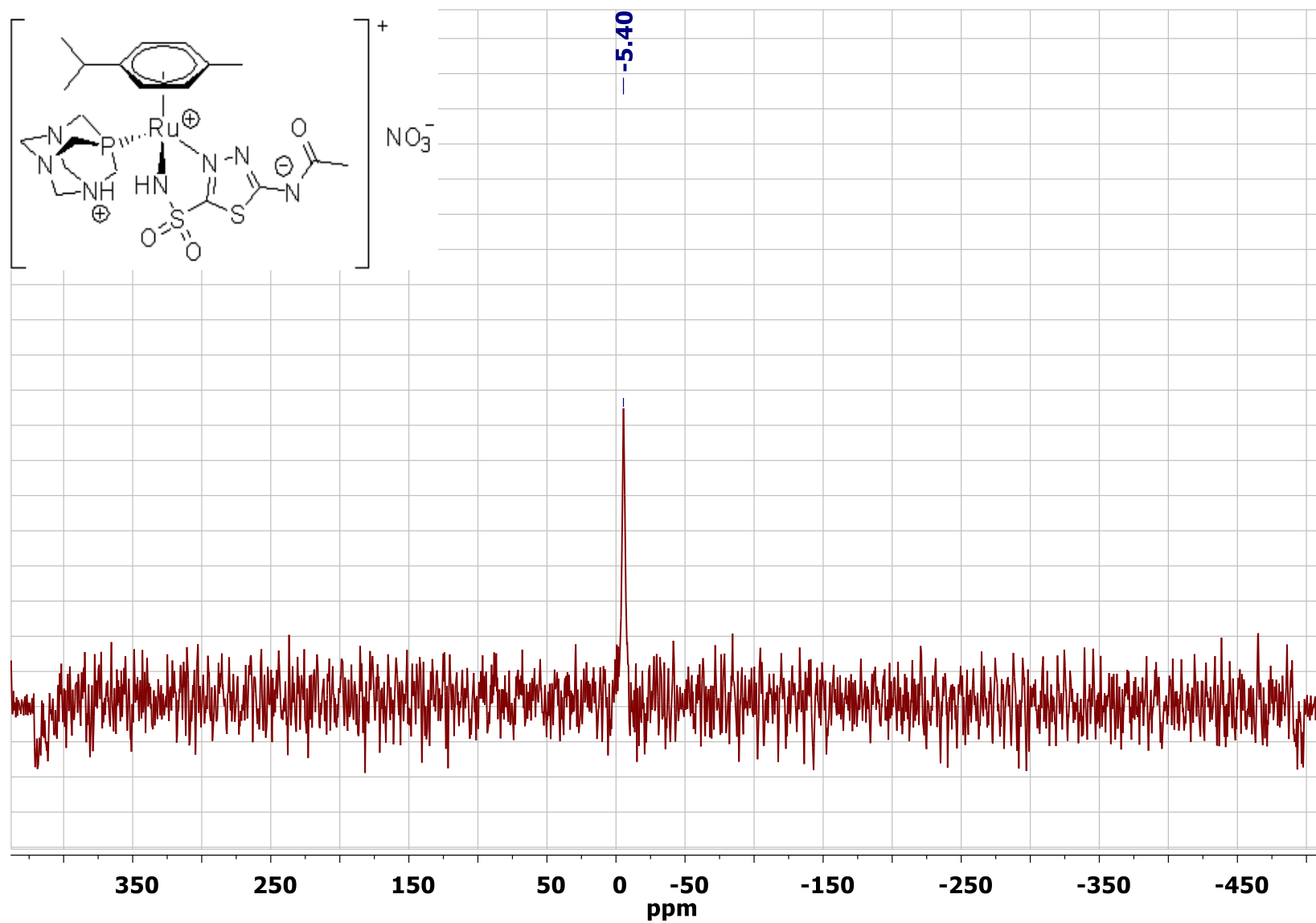


Figure S33. $^{31}\text{P}\{^1\text{H}\}$ NMR spectrum (162 MHz, CD_3OD) of $[(\eta^6\text{-}p\text{-cymene})\text{Ru}(\kappa^2\text{N}^8, \text{N}^{10}\text{-Acsm})(\kappa\text{P-ptaH})]\text{NO}_3$, $[\text{6}]\text{NO}_3$ ($\text{H}_2\text{O}/[\text{6}]^+$ mol. ratio ≈ 13 mol. ratio 14).

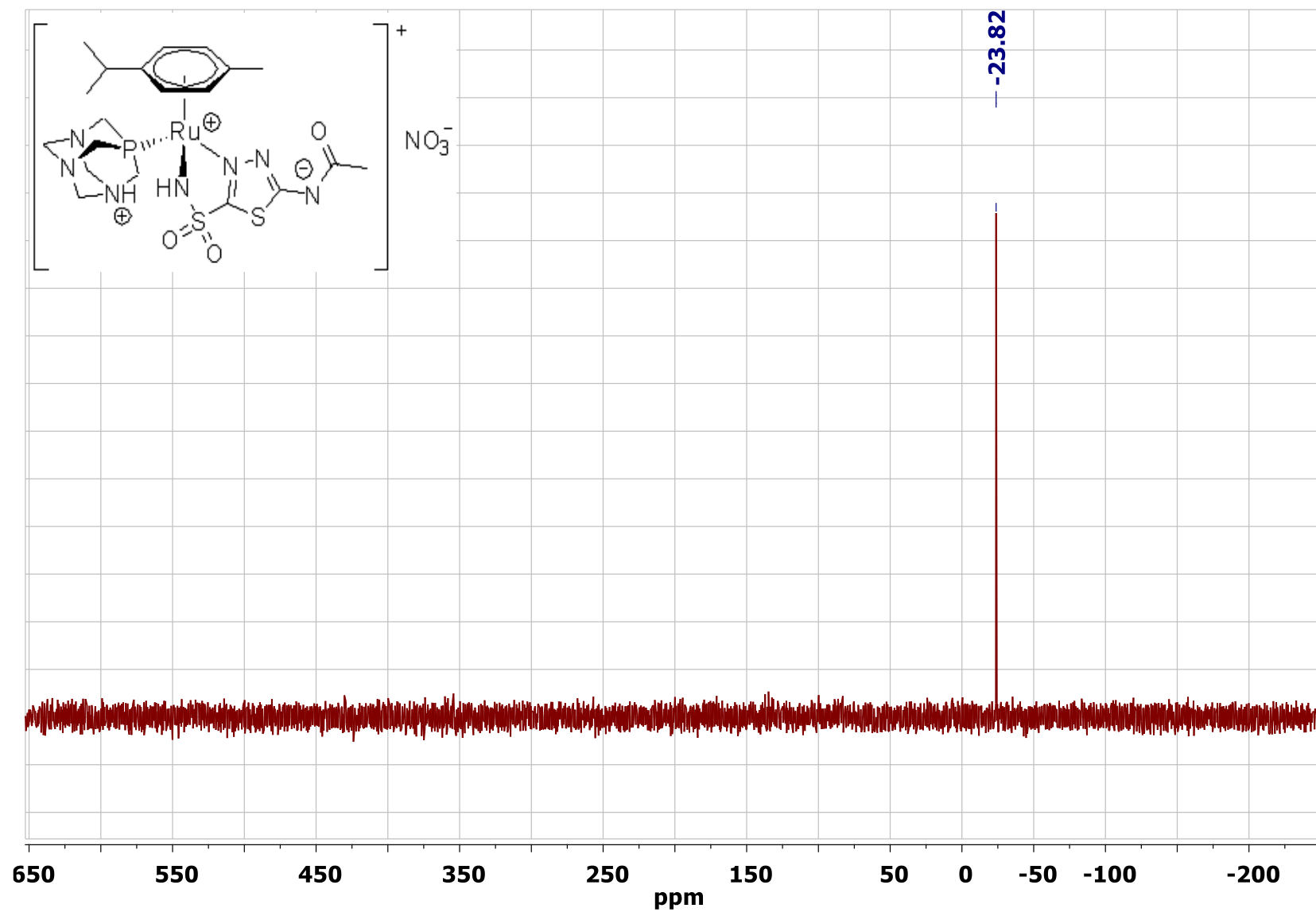


Figure S34. ^1H NMR spectrum (401 MHz, CD_3OD) of $[(\eta^6\text{-}p\text{-cymene})\text{Ru}(\kappa^2\text{N}^6, \text{N}^{10}\text{-Acm})(\kappa\text{P}\text{-ptaH})][\text{TsO}]$, $[\text{6}][\text{TsO}]$ ($\text{H}_2\text{O}/[\text{6}]^+$ mol. ratio ≈ 9 mol. ratio 14).

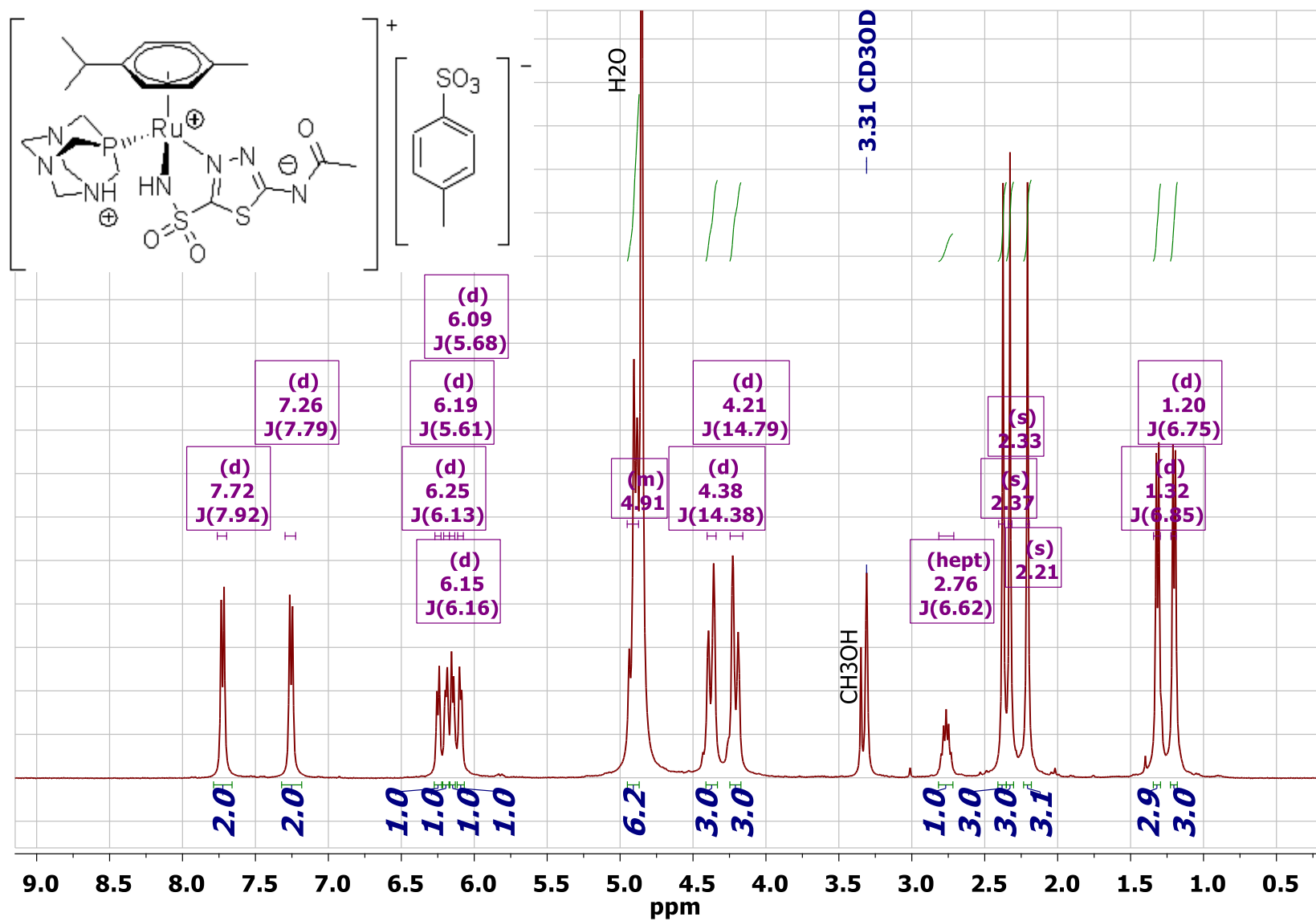


Figure S35. $^{13}\text{C}\{^1\text{H}\}$ NMR spectrum (101 MHz, CD_3OD) of $[(\eta^6\text{-}p\text{-cymene})\text{Ru}(\kappa^2\text{N}^8, \text{N}^{10}\text{-Acm})(\kappa\text{P-ptaH})][\text{TsO}]$, $[\text{6}][\text{TsO}]$ ($\text{H}_2\text{O}/[\text{6}]^+$ mol. ratio ≈ 9 mol. ratio 14).

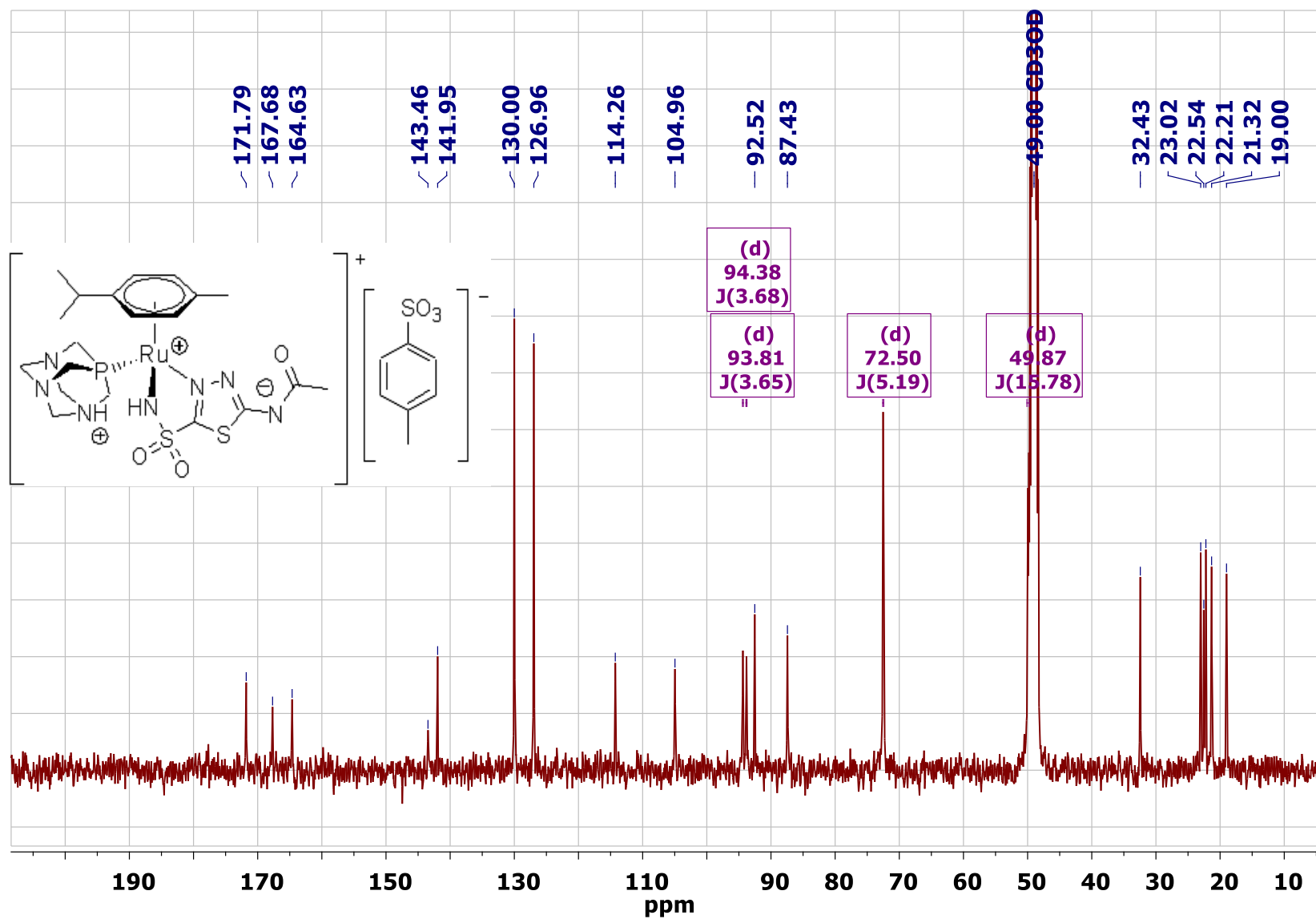
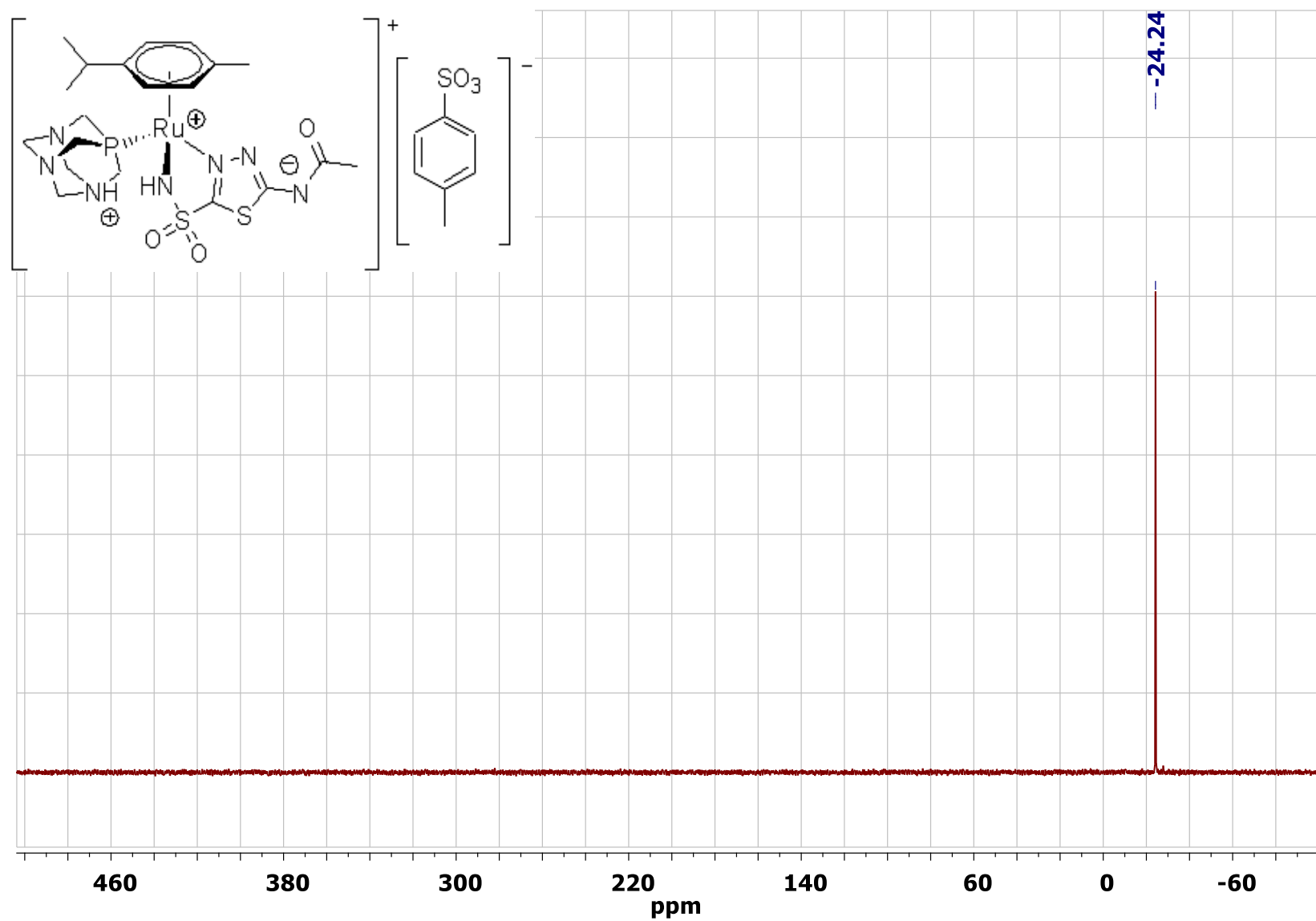


Figure S36. $^{31}\text{P}\{^1\text{H}\}$ NMR spectrum (162 MHz, CD_3OD) of $[(\eta^6\text{-}p\text{-cymene})\text{Ru}(\kappa^2\text{N}^8, \text{N}^{10}\text{-Acm})(\kappa\text{P-ptaH})][\text{TsO}]$, **[6][TsO]** ($\text{H}_2\text{O}/[\text{6}]^+$ mol. ratio ≈ 9 mol. ratio 14).



Notes and references

- 1 Both structures are depicted since, to the best of our knowledge, the crystal structure of sodium acetazolamidate or other alkali metal salt has not been reported. Concerning NMR data in DMSO, the structure with negative charge on N6 (acetamide) seems more likely: the N6-H signal falling at *ca.* 11 ppm in Ac_mH₂ was not present in the spectrum of Na[Ac_mH] while the signal at 7.6 ppm due to the sulfonamide group (N1-H; 8.2 ppm in Ac_mH₂) integrates for two protons.
- 2 The signal was attributed to the carbonyl carbon due to a ¹H-¹³C correlation with the methyl protons (2.22 ppm) observed in the *gs*-HMBC experiment. The same signal was previously attributed to a carbon belonging to the 1,2,5-thiadiazole ring. H. Loghmani-Khouzani, T. Rauckyte, B. Ośmiałowski, R. Gawinecki, E. Kolehmainen, *Phosphorus, Sulfur, and Silicon*, 2007, **182**, 2217–2225.
- 3 Calculated by using the formula pD = pH* + 0.4, where pH* is the value measured for H₂O-calibrated pH-meter. (a) C. C. Westcott, pH Measurements; Academic Press: New York, 1978. (b) A. K. Covington, M. Paabo, R. A. Robinson, R. G. Bates, *Anal. Chem.*, 1968, **40**, 700-706.
- 4 T. Rundlöf, M. Mathiasson, S. Bekiroglu, B. Hakkarainen, T. Bowden, T. Arvidsson, *J. Pharm. Biomed. Anal.*, 2010, **52**, 645–651.
- 5 Fulmer, G. R.; Miller, A. J. M.; Sherden, N. H.; Gottlieb, H. E.; Nudelman, A.; Stoltz, B. M.; Bercaw, J. E.; Goldberg, K. I. NMR Chemical Shifts of Trace Impurities: Common Laboratory Solvents, Organics, and Gases in Deuterated Solvents Relevant to the Organometallic Chemist, *Organometallics*, 2010, **29**, 2176–2179.
- 6 Including other unidentified {(*p*-cymene)Ru} species with signals in the 6.07-5.95 ppm range as [2^S]⁺.
- 7 S. Otto, A. Ionescu, A. Roodt, *J. Organomet. Chem.*, 2005, **690**, 4337–4342.
- 8 The ¹H NMR set of signals for **5** in D₂O (**e**) and that found in the D₂O + PBS solution (**f**) are rather similar, except for the arene (6.11 (d, 1H), 6.07 (m, 2H), 6.00 (d, 1H) in **e**; 6.09 (m, 3H), 5.98 (d, 1H) in **f**) and the acetamide (2.30 ppm in **e**, 2.25 in **f**) resonances.
- 9 (a) L. Biancalana, S. Zacchini, N. Ferri, M. G. Lupo, G. Pampaloni, F. Marchetti, *Dalton Trans.*, 2017, **46**, 16589-16604; (b) M. Patra, T. Joshi, V. Pierroz, K. Ingram, M. Kaiser, S. Ferrari, B. Spingler, J. Keiser, G. Gasser, *Chem. Eur. J.*, 2013, **19**, 14768–14772.
- 10 (a) M. Stebler-Rothlisberger, A. Ludi, *Polyhedron*, 1986, **5**, 1217-1221. (b) L. Bíró, E. Farkasa, P. Buglyó, *Dalton Trans.*, 2012, **41**, 285-291.

-
- 11 Adding water to a solid mixture of **[4]**NO₃ and **[6]**NO₃ was not suitable for the purpose of this experiment. Indeed, by doing so, one of the two components (presumably **[4]**NO₃, judging by the ¹H NMR spectrum) did not dissolve completely even after 72 h at 37°C.
- 12 The set of ¹H NMR signals after Na₂CO₃ addition matched that observed for **5** in the D₂O + PBS solution (**f**). Small discrepancies are probably due to the different pH of the two solutions.
- 13 The chemical shift in the ³¹P{¹H} NMR spectrum ($\delta/\text{ppm} = -23.5$) clearly indicates that protonation occurred on the pta ligand, as in **[6]**⁺. The ¹H NMR spectrum after HNO₃ addition do not match that of **[6]**⁺ in D₂O, however this may be due to the different pH of the two solutions.
- 14 ¹H, ¹³C{¹H} and ³¹P{¹H} NMR resonances of **[6]**⁺ in CD₃OD (either **[6]**NO₃ and **[6]**[TsO]) are dependent on the amount of water in the solvent, more precisely on the water:**[6]**⁺ molar ratio (calculated by ¹H NMR on the basis of arene protons and water peak, considered as HDO).